last Copy

HEAT TRANSFER DURING FILM CONDENSATION OF A LIQUID METAL VAPOR

Suhas P. Sukhatme
Warren M. Rohsenow

April 1964

Report No. 9167-27
Department of
Mechanical Engineering
Massachusetts Institute
of Technology

Contract No. AT (30-1)-2995
AEC Code: Report MIT - 2995 - 1

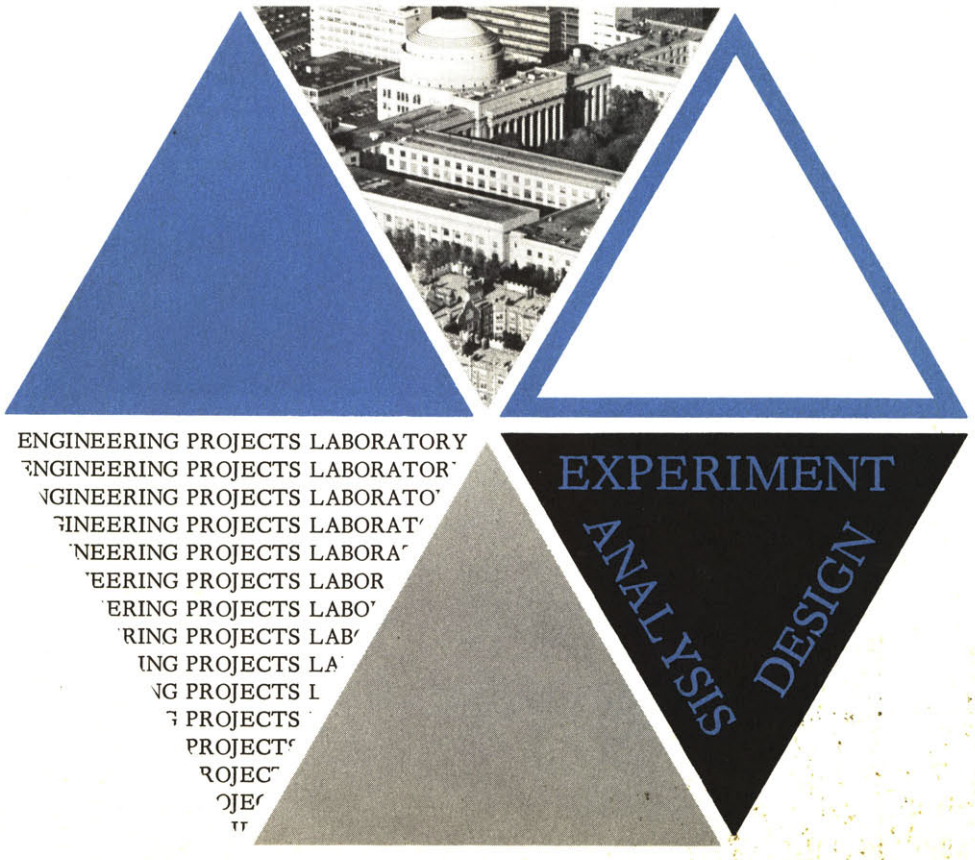

TECHNICAL REPORT NO. 9167-27

HEAT TRANSFER DURING FILM CONDENSATION OF A LIQUID METAL VAPOR

by

Suhas P. Sukhatme

Warren M. Rohsenow

Sponsored by the U. S. Atomic Energy Commission

Contract No. AT (30-1)-2995

AEC Code: Report MIT-2995-1

April 1964

Department of Mechanical Engineering

Massachusetts Institute of Technology

Cambridge 39, Massachusetts

ABSTRACT

The object of this investigation is to resolve the discrepancy between theory and experiment for the case of heat transfer during film condensation of liquid metal vapors. Experiments by previous investigators have yielded data which are extremely scattered and markedly below the predictions of both the classical Nusselt theory and more recent modifications to it.

All theoretical treatments so far have taken account only of the thermal resistance presented by the condensed film. However, calculations from kinetic theory show that with liquid metals a significant thermal resistance can exist at the liquid-vapor interface. This resistance increases with decreasing vapor pressure and is dependent on the value of the "condensation coefficient." Experimental work to back up this hypothesis of a liquid-vapor interfacial resistance is presented. The working fluid for the experiments is mercury condensing at low pressures in the absence of non-condensable gases on a vertical nickel surface.

Data of previous investigators are analyzed, and possible reasons for being unable to interpret these results meaningfully are cited.

TABLE OF CONTENTS

I. INTRODUCTION

In recent years, liquid metals have begun to find increasing use as heat transfer media both in single-phase and in change-of-phase processes. They have high thermal conductivities and low Prandtl numbers and remain liquids over wide ranges of temperature. This makes them uniquely suitable for high heat flux, high temperature applications. They are being used in nuclear reactors, in conventional power plant cycles, and in various space power generation programs, e.g., SNAP.

This investigation is concerned with the process of heat transfer during film condensation of liquid metal vapors. The general observation of all previous experimental investigations has been that the measured values of the heat transfer coefficient on the condensing side are much lower than the predictions from Nusselt's classical theory or from more recent modifications to that theory. No explanation of the reasons for this discrepancy has so far been made.

From a practical as well as a fundamental viewpoint, it would be useful to remove the disagreement and to understand the reasons for its existence. This is the object of the research investigation reported here.

Review of the Literature

Development of the Theory

The specific problem under consideration will be the case of film condensation of a stationary, pure, saturated vapor on an isothermal

vertical surface. The first formulation of the problem is due to Nusselt,[1] who made the following assumptions:

(i) The only significant thermal resistance to the condensation process is presented by the liquid condensate film. The temperature of the liquid at the liquid-vapor interface is, therefore, the saturation temperature corresponding to the pressure in the vapor space.

(ii) The condensate flow is laminar.

(iii) The fluid properties are constant.

(iv) Subcooling of the condensate may be neglected.

(v) Momentum changes through the condensate are negligible; i.e., there is essentially a static balance of forces.

(vi) The stationary vapor exerts no drag on the downward movement of the condensate.

(vii) The temperature distribution in the film is linear. He derived the well-known formula:

$$h_{Nu} = 0.943 \sqrt[4]{\frac{g \rho_l^2 k^3 \lambda'}{\mu L \cdot \Delta T_f}} \qquad (1)$$

where $\lambda' = \lambda$, the latent heat of vaporization.

Seban[2] has extended Nusselt's analysis for the case of higher Reynolds numbers by assuming a transition from laminar to turbulent flow at a Reynolds number of 1600 and a universal velocity distribution in the film. His results verify the qualitative expectation that heat transfer coefficients should increase for common fluids (Pr $\approx$ 0.5 or greater) but should not for low Prandtl number fluids because of high

values of thermal diffusivity as compared to the turbulent diffusion coefficient for heat.

Nusselt's analysis has been extended by Bromley,[3] who included effects of subcooling of the condensate, and by Rohsenow,[4] who allowed for non-linearities in the film temperature distribution. In equation (1), Rohsenow showed $\lambda' = \lambda + 0.68 C_p \Delta T_f$. These refinements become important only at high values of $C_p \Delta T_f / \lambda$. Actually in most applications this parameter has a value between 0 and 0.2.

Sparrow and Gregg[5] have solved the boundary layer equations for a laminar film through a similarity transformation, thus taking account of momentum changes. For common fluids their results follow Nusselt's prediction closely, but for low Prandtl number fluids the heat transfer coefficient drops below the Nusselt prediction with increasing $C_p \Delta T_f / \lambda$. Mabuchi[6] has obtained substantially the same results by an integral method.

Recently Chen,[7] Koh, Sparrow and Hartnett,[8] Koh,[9] and Chato[10] have almost simultaneously considered the effect of the vapor drag. Their results indicate little disagreement with Nusselt's theory for common fluids. For low Prandtl number fluids, however, the heat transfer coefficient is found to drop a little below that determined by Sparrow and Gregg.

All these analytical results are of the form

$$\frac{h_{Nu} L / k}{0.943 \sqrt[4]{\frac{g L^3 P_r}{\nu^2}}} = F\left(\frac{C_p \Delta T_f}{\lambda} , P_r\right)$$

where the function F is slightly different for each of the analyses.

Thus the latest refinements to Nusselt's analysis have removed the restrictions of assumptions (iv), (v), (vi), and (vii). All of them, however, retain assumption (i). Figure 1 illustrates the results of the above[1,7,8,9,10] theoretical investigations.

Experimental Investigations for Liquid Metals

Although experiments have substantially borne out the theoretical predictions for common liquids ($Pr \geq 0.5$),[11] the same cannot be said for liquid metals. Data on liquid metal condensation are scarce. Only three investigations, which approximate the conditions of the above theory, are available in the literature. The investigators are Misra and Bonilla,[12] Cohn,[13] and Roth.[14] They have worked with mercury and sodium, mercury and cadmium, and rubidium respectively. The fluids have been condensed on the outside or inside of vertical tubes. Their data are presented in non-dimensional form in Figure 1. Correlations suggested by them are also drawn.

In addition to these investigations for a stagnant vapor, the data of General Electric[15][16] (condensation of flowing potassium vapor inside a horizontal tube) and of Broglio et al[17] (condensation of flowing sodium vapor inside a vertical tube) are also available. These results too are lower than any theoretical estimates. Since they are not directly applicable to the problem under consideration, they are not plotted.

Although the experimental results in Figure 1 are quite scattered, a number of important conclusions can be drawn from them.

(i) The measured values of the condensing side heat transfer coefficient are always lower than the predictions of Nusselt's theory

or modifications to it. Sometimes the measured values are lower by as much as two orders of magnitude.

(ii) Since lines of constant heat flux are inclined with a slope of -1 on an h - ΔT log-log plot (such as in Figure 1), the lines drawn through the data, which are also approximately inclined at a slope of -1, cannot possibly be acceptable correlations for condensation. During condensation, we must expect the heat flux to be dependent on a temperature drop. The suggested correlations are merely lines of constant heat flux and indicate the average value of the heat flux around which the investigator concerned has worked.

(iii) Further, the falling of the data along lines of constant heat flux indicates the presence of a thermal resistance (additional to that prescribed by present theory) in the path of the condensing vapor. This additional resistance has varied from test to test.

The reason why Misra and Bonilla's mercury data for air- and water-cooled condensers fall so far apart is obvious from (ii) and (iii). The air data are for much lower heat fluxes.

It is clear that we must now consider the various ways in which an additional thermal resistance can interpose itself between the condensing vapor and the condenser wall.

Before passing on to this, it is worth mentioning that Dukler[18] has recently suggested a theory which seems at first glance to agree well with some of Misra and Bonilla's data. An examination of the simplifying assumptions made by Dukler quickly reveals that this agreement

can only be fortuitous. In the outer region of the film, Dukler has made the assumption that the molecular heat transport coefficient is negligible in comparison to the turbulent eddy coefficient (refer to Appendix of his paper). This assumption is reasonable for high Prandtl number fluids, but is totally unjustifiable for Prandtl numbers of the order of 0.01, particularly at Reynolds numbers of the order of 1000. Sample calculations show that by not making this assumption, Dukler's results would fall close to Nusselt's in the laminar region.

Subsequently Lee,[19] using a different numerical procedure but the same physical model as Dukler's, has solved the problem correctly. As is to be expected from the model, he has obtained results which essentially smooth out the discontinuity between Nusselt's laminar theory and Seban's theory for the turbulent film, and the magnitudes agree with the Nusselt and Seban results.

II. ANALYTICAL CONSIDERATIONS

It is useful at this stage to consider the behaviour of a system in which a pure saturated vapor at pressure p_v and temperature T_v is being boiled and condensed. Consider the closed system (Figure 2) in which q units of heat per unit of time are being introduced into the liquid. A condenser tube is inserted into the system, and its wall is maintained at a temperature T_w by running a coolant through it at a suitable rate. All other parts of the system are well insulated, so that all the heat q has to be taken away through the condenser surface.

If the condensate film alone offers thermal resistance to the condensing vapor and it has a thickness δ as prescribed by present theories,[7,8,9,10] the appropriate temperature distribution will be as shown in Figure 3 (a). The liquid-vapor interface will take on a temperature T_s which can be calculated from theory. This temperature will extend everywhere into the vapor space ($T_v = T_s$), and the pressure p_v in the system will be the saturation pressure corresponding to it.

If, on the other hand, other thermal resistances are present, we would have the temperature distribution shown in Figure 3(b). An additional resistance can occur

(i) at the liquid-vapor interface,

(ii) because of a film thickness greater than that predicted by theory,

(iii) at the solid-liquid interface, and

(iv) in the vapor space when non-condensable gases are added to the pure vapor.

We now consider each of these individually.

The Liquid-Vapor Interface

We are concerned in this section with a pure saturated vapor at pressure p_v and temperature T_v condensing on its own liquid phase, whose surface temperature is T_s. The phenomenon of such an interphase mass transfer is viewed from the standpoint of kinetic theory as a difference between two quantities--a rate of arrival of molecules from the vapor space towards the interface and a rate of departure of molecules from the surface of the liquid into the vapor space. When condensation takes place, the arrival rate exceeds the departure rate. During evaporation the reverse occurs, and during an equilibrium state the two rates are equal.

Clearly, in order to maintain a net rate of transfer towards the interface during condensation, an interfacial temperature drop must exist. The question arises: Is this temperature drop always insignificant compared to the drop across the condensate film (assumption (i) of Nusselt's theory)? Or are there some circumstances when the interfacial drop may be important? In order to answer these questions, we need a quantitative description of the process. The treatment that follows is essentially due to Schrage.[20]

Using a Maxwell-Boltzmann distribution, it can be shown that in a stationary container of molecules, the rate of flow of mass (molecules) passing in either direction (to the right or to the left) through an imagined plane is given by

$$m\frac{N}{A} = \left(\frac{M}{2\pi \bar{R}}\right)^{1/2} \cdot \frac{p}{T^{1/2}} \qquad (2)$$

where

N/A = flux of molecules, number per unit time per unit area

m = mass of a molecule

M = molecular weight

$\bar{R}$ = universal gas constant, and

p and T are the pressure and temperature.

If there is a progress velocity V_y toward the plane ($w/A = \rho V_y$), then

$$m\frac{N}{A} = \left(\frac{M}{2\pi\bar{R}}\right)^{1/2} \cdot \frac{p}{T^{1/2}} \cdot \Gamma \qquad (3)$$

where $$\Gamma = e^{-\phi^2} + \phi\pi^{1/2}\left[1 + \operatorname{erf}\phi\right] \qquad (4)$$

$$\phi = \frac{V_y}{(2\bar{R}T/M)^{1/2}} = \frac{w/A}{\rho\,(2\bar{R}T/M)^{1/2}} \qquad (5)$$

At a liquid-vapor interface not all of the molecules striking the surface will actually condense. We define σ as that fraction of the molecules striking the surface which actually do condense. The quantity σ is called the condensation coefficient. In a similar way we may define an evaporation coefficient σ_e, which is the ratio of the flux of molecules actually leaving a surface to the flux given by Equation (2).

At a condensing surface, Schrage[20] visualizes the pure saturated vapor stream at T_v moving toward the surface at a progress flow rate of w/A and a counter flow of molecules at T_s from the surface as being the flow equivalent to molecules in a stationary container. Then from Equations (2) and (3) with σ and σ_e, the net mass flux toward the liquid-vapor interface is expressed as follows:

$$\frac{w}{A} = \left(\frac{M}{2\pi \bar{R}}\right)^{1/2} \left\{ \sigma \Gamma \frac{p_v}{T_v^{1/2}} - \sigma_e \frac{p_s}{T_s^{1/2}} \right\} \qquad (6)$$

where w/A is in mass units per unit time per unit area, p_v and T_v are the pressure and temperature of the pure saturated vapor in the bulk space, T_s is the temperature of the liquid at the liquid-vapor interface, and p_s is the saturation pressure corresponding to T_s. The quantity ϕ (which is needed for calculating Γ) is given by equation (5), in which ρ and T are replaced by ρ_v and T_v. It should be noted that this superposition of flow rates, toward and away from the condensing surface, neglects the intraphase heat transfer.

At equilibrium when there is no net condensation (w/A = 0), then $T_v = T_s$ and $p_v = p_s$, also $\phi = 0$ and $\Gamma = 1$. Clearly, at equilibrium $\sigma_e = \sigma$. Under non-equilibrium conditions with net condensation, if it is assumed that the condensation and evaporation coefficients are still equal, then Equation (6) becomes

$$\frac{w}{A} = \sigma \left(\frac{M}{2\pi \bar{R}}\right)^{1/2} \left\{ \Gamma \frac{p_v}{T_v^{1/2}} - \frac{p_s}{T_s^{1/2}} \right\} \qquad (7)$$

Equation (7) shows that for any given fluid and a specified mass transfer rate, the interfacial temperature drop $(T_v - T_s)$ increases with decreasing pressure p_v and with a decreasing value of the coefficient σ.

Equation (7) can be simplified with the help of the Clausius-Clapeyron relation and put in the form:[21]

$$\frac{w}{A} = \left(\frac{\sigma}{2-\sigma}\right)\left(\frac{2}{\pi}\right)^{1/2}\left(\frac{M}{\bar{R}}\right)^{3/2}\frac{p_v \lambda}{T_v^{5/2}}\,(T_v - T_s) \qquad (8)$$

This simpler version permits the interfacial resistance concept to be expressed in convenient non-dimensional form.[22] However, the use of equation (8) is restricted to instances where the quantity ϕ is less than 0.1 and the temperature difference $(T_v - T_s)$ is small. In many tests in this investigation, these conditions have not been obeyed. Hence for the sake of generality and accuracy, equation (7) is used.

The Condensation Coefficient

The condensation coefficient σ must be clearly distinguished from the condensing heat transfer coefficient. σ can only take on values in the range 0 to 1. The history of the experiments to determine the values of σ for various substances is instructive. In nearly all cases the initial experiments gave values much less than unity. With several substances, however, when great care was taken to have the substances completely clean and pure and to have accurate measurements, higher values of σ were obtained. In some instances values of unity were finally obtained.

In the case of mercury Hertz[23] obtained a value of 1/9. Knudsen[24][25] initially measured a value of 0.0005. On repeating his experiments with a purer sample of mercury, he obtained a value close to that of Hertz. Subsequently on using the purest mercury he could prepare, he obtained a value of unity. Volmer and Estermann[26] also obtained a value close to unity.

In the case of water a large number of investigators seem to agree on a value of about 0.04. A comprehensive compilation of condensation coefficients for a large number of substances is given by Paul.[27]

It is clear that for any particular fluid, unless we have some specific knowledge to the contrary, there is no reason to presume that the condensation coefficient should take on a value of unity. In fact, judging from the experience of previous experimenters, in any large engineering system where it is hard to maintain a high degree of purity, a value of σ less than unity seems more probable.

Magnitude of the Interface Temperature Drop

In the following table the temperature drop at the liquid-vapor interface is calculated for water, mercury, and sodium at vapor pressures of 760 mm, 100 mm, and 10 mm. The calculation is done for a temperature drop across the condensate film of 5 ^{o}F. From Equation (1), with L assumed to be 0.5 ft., the magnitude of h_{Nu} is calculated. Then $q/A = h_{Nu} (T_s - T_w) = 5\, h_{Nu}$ and $w/A = (q/A)/\lambda'$ from an energy balance. With this value of w/A, $(T_v - T_s)$ is determined from Equations (7) or (8), assuming $\sigma = 1$ and 0.04 for water, $\sigma = 1$ and 0.1 for mercury and $\sigma = 1$ for sodium.

	Assumed value of σ	$(T_v - T_s)$ °F with pressure of			Mass flux from Nusselt's theory (lbm/hr-ft^2)
		760 mm	100 mm	10 mm	
Water	1.0	0.003	0.01	0.1	7.9
	0.04	0.1	0.7	4.8	
Mercury	1.0	0.3	1.6	10.0	1115
	0.1	5.9	29.6	Pressure is below min. value	
Sodium	1.0	0.6	2.8	18.0	250

With these numerical values we are in a position to answer the questions posed earlier regarding the significance of the interfacial resistance. We see that:

(1) For any fluid under conditions of a low enough pressure and/or low value of σ, the interfacial resistance represented by the drop $(T_v - T_s)$ can become significant. Attention has previously been drawn to this fact by Silver,[28] who has done similar calculations for water.

(2) Under conditions of the same film drop, same vapor pressure, and same value of σ, the drop $(T_v - T_s)$ for a liquid metal is much higher than that for a commonly used fluid like water. This is primarily due to the fact that (i) for the same pressure, the liquid metal has a much higher saturation temperature, and (ii) the liquid metal has a higher thermal conductivity.

The Solid-Liquid Interface

The thermal resistance at a solid-liquid interface was first noted by experimenters in the study of heat transfer to liquid metals flowing in tubes. It is ascribed to the presence of oxide layers and/or adsorbed gas layers on the tube surface. The presence of such layers in turn prevents the flowing liquid metal from wetting the tube metal surface. It is only when the liquid metal has "eaten" through the oxide and gas layer, removed it, and come into contact with the bare metal tube that wetting finally occurs. In some instances it is known that the liquid metal goes on to interact with the tube metal and forms some kind of an intermetallic film, which usually has no significant thermal resistance.

In general, it may be stated that when the surface is known to be wetted, a thermal resistance at the interface is not observed. Hence during film condensation, a significant thermal resistance at the solid-liquid interface seems unlikely. This does not imply that a significant resistance has to exist with non-wetting.

For the particular case of mercury flowing over nickel (which we plan to use in our experiments), Kirillov et al[29] have reported the absence of a thermal resistance at the interface "apparently because of some interaction between nickel and mercury."

Condensate Film Thickness Greater Than That Predicted by Theory

The fluid mechanics of the condensate film appears to have been exhaustively treated, and there seems no reason to expect a film which is much thicker than that predicted by current theory. We shall not

explore this possibility analytically, but will rely on the experiments to prove or disprove the present predictions.

The Effect of Non-Condensable Gases

Unlike the three previous resistances whose presence may be unavoidable, the thermal resistance due to the presence of non-condensable gases can be eliminated with proper care. Very small amounts of non-condensable gases in the bulk space are known to decrease the heat transfer coefficient considerably because they produce a resistance to diffusion of the condensing vapor towards the liquid-vapor interface. For this reason their presence has always plagued experimental work in condensation. It is instructive, therefore, to note certain well-known manifestations of the presence of such gases in an experimental system.

Consider again the closed system of Figure 2. For a particular heat flux and condenser wall temperature and in the absence of non-condensable gases, let the saturation pressure and temperature in the vapor space be p_v and T_v. If now a small amount of non-condensable gas is introduced into the system, the pressure will increase to a value which is the sum of the partial pressures of the condensing vapor and the non-condensable gas. The partial pressure of the condensing vapor in the bulk space will by itself be greater than the previous value. Also, the temperature in the bulk space will now correspond on the saturation curve to the partial pressure of the condensing vapor. The resulting data will yield a lower heat transfer coefficient at an increased pressure.

It is quite clear that should non-condensable gases be present in significant quantities without the experimenter's knowledge, their effect

superposed on the liquid-vapor interface resistance would yield data devoid of any meaning.

The discussion thus far has shown that in the case of a liquid metal vapor, condensing as a film in the absence of non-condensable gases, the probability of having a significant thermal resistance at the solid-liquid interface is small. Because of previous experimental evidence,[29] this probability is even smaller with a nickel-mercury system. Also, it does not seem likely that the condensate film is much thicker than that prescribed by current theory. The only possibility for an additional resistance exists at the liquid-vapor interface. Here the thermal resistance may be very significant and even dominant, particularly at low pressures and/or with low values of the condensation coefficient.

III. EXPERIMENTAL INVESTIGATION

Description of the Apparatus

A drawing and photographic view of the system is shown in Figures 4 and 5. The apparatus was a closed welded boiler-condenser system made of stainless steel 304. The boiler was a cylindrical shell (5 in. schedule 5 pipe; 15 in. long) with a 1/2-in. pipe at the top through which the vapor flowed into the condensing chamber. Watlow electric heaters capable of giving upto 6-1/2 KW of heat were wrapped around the shell and inserted through wells in the boiler base. Fill and drain lines were welded to the boiler and could be closed by Hoke stainless steel sealed bellows valves. The boiler was filled with approximately 120 lbs. of clean mercury.

The condensing chamber was made from 6 in. schedule 5 pipe, 11 in. long. It had a cup shape welded at the bottom. A 1/2-in. pipe line returned the condensate to the boiler. The condensation took place on a vertical nickel tube (3/4 in. dia.; 6 in. long) inserted through a Conax packing gland with a "lava" sealant. Two 2 in. dia. Vycor glass windows with graphitized asbestos gaskets were provided in the walls of the condensing chamber to permit observation of the condensation process. In order to prevent leakage through the windows into the condensing chamber, a jacket was provided around it. This jacket was at all times evacuated to a pressure below that in the condensing chamber.

The top of the condensing chamber led through an ice trap and a chemical cartridge (which absorbed traces of mercury vapor) to a vacuum

pump. An essential feature of the design was the care taken to make it tight and leak-proof. There were few mechanical joints or seals. The system was designed to eliminate any places where non-condensable gas would be trapped, thus permitting any leakage to be swept quickly upwards and purged.

The 6 in. long nickel tube condenser was of the double tube, bayonet type. The choice of nickel for the condenser surface was based on Misra and Bonilla's observation that it was relatively easy to obtain film condensation of mercury on it. The cooling fluid (water or Dow Corning 200, 2 cs silicone oil) entered through the 1/2 in. O. D. inner tube, flowed down to the bottom of the condenser, and then upwards and out through the annulus. A closed circulating pumping system was used with the silicone oil. The object of using the silicone oil was to obtain the higher wall temperatures without pressurizing.

Measurements

Temperatures

The following temperatures were measured:

(i) Temperature of the mercury vapor in the boiler.

(ii) Temperature of the mercury vapor in the condensing chamber.

(iii) Temperature of the air in the jacket around the condensing chamber (at three locations along the periphery).

(iv) Temperatures of the cooling fluid prior to entering the condenser.

(v) Difference of temperature between the outlet and inlet temperatures of the cooling fluid.

Temperatures (i), (ii), and (iii) were measured with 20 gage, iron-constantan thermocouples supplied with a calibration correction by the manufacturer. Temperatures (iv) and (v) were measured with calibrated copper-constantan thermocouples. (v) was a two-junction thermopile. All e.m.f. measurements were made on a precision Rubicon potentiometer capable of reading upto 1 μV.

(vi) The average temperature of the condenser wall was determined from a precise measurement of the electrical resistance of a section of the nickel tube. The technique is discussed in Appendix I.

Pressures

The pressure in the condensing chamber was measured with a Cenco Mcleod gage which could read upto 18 mm. The smallest division on the scale was 0.2 mm., and the accuracy of the measurement is estimated to be $\pm$ 0.05 mm.

In addition the pressures in the line leading from the ice trap to the vacuum pump and in the jacket around the condensing chamber were read on vacuum gages (range 0-30 in.; smallest division 0.1 in.).

Condensate Film Thickness

The film thickness was measured at various positions along the length of the condenser by means of a gamma ray attenuation technique, which is discussed in Appendix II. By assuming a linear temperature profile in the film, the heat transfer coefficient based on the film thickness can be calculated from this measurement.

Coolant Flow Rate

A rotameter (Flowrator Series 10A2700; 1 in. tube with a stainless steel 1-GSVT-64 float; Fischer and Porter Co.) was used to measure the

coolant flow rate. A water calibration was supplied by the manufacturers. The meter can be used for any fluid so long as the fluid properties fall below a "viscosity ceiling factor." The water calibration curve for the meter was checked by weighing water collected over a known length of time. The measurement of the flow rate is believed to be accurate to at least $\pm$ 2%.

Electric Currents

The currents fed to the heaters were recorded. Since the resistances of the heaters were known, the quantity of electrical power supplied to the boiler could be calculated from this measurement.

The Condensing Side Heat Transfer Coefficient

The condensing side coefficient is given by

$$h_c = \frac{q/A}{(T_v - T_w)} \tag{9}$$

where q/A = average heat flux

T_v = saturation temperature corresponding to pressure p_v in the bulk vapor space

T_w = temperature on the outer surface of the condenser wall

The average heat flux was calculated from the coolant flow rate and rise of temperature. An approximate check was obtained by calculating the electrical heat input. The temperature T_v, which corresponded to the measured pressure p_v, was approximately checked against the measured temperature in the vapor space. The temperature corresponding to p_v was used in equation (9) instead of the measured value because the vapor

in the condensing chamber was slightly superheated. T_w was obtained by calculating to the outer surface knowing the average temperature of the condenser tube from the electrical resistance measurement, the heat flux, and the thermal conductivity and thickness of the nickel wall. The value of T_w was approximately checked against a value obtained by using a forced convection heat transfer correlation on the cooling side.

Because of these checks on each of the quantities involved in equation (9), we conclude that there is no significant error in the value of the condensing side heat transfer coefficient.

Safety Procedures

In any apparatus involving the use of mercury vapor, the experimenter must guard against two possibilities: (i) poisoning due to the sudden escape of vapor from its containing vessel because of an accident; (ii) chronic poisoning due to the continuous slow leakage of the vapor from the apparatus.

In this investigation the following precautions were taken:

(1) The apparatus was located in a test cell to which there were two exits. A quick exit was possible, and the doors provided a fairly good seal. The air in the room was continuously exhausted through duct work leading to the top of the building.

(2) The part of the system in which the mercury was boiled and condensed was almost entirely made of stainless steel 304. It was fitted with special stainless steel Hoke valves and was essentially an all-welded construction. The system was pressurized and tested for leaks before the mercury was initially poured in.

(3) In all the experiments the system pressure was below atmospheric. Leakage (if it did occur) was, therefore, in an inward direction.

(4) A mercury vapor detector (Mine Safety Appliances), which detected low concentrations of mercury vapor in air, was used during each test to insure that the existing concentration in the vicinity of the apparatus was below the recommended safe level viz. 0.1 milligrams of mercury per cubic meter of air.

(5) The experimenter was provided with a gas mask (Mine Safety Appliances Mersorb Respirator) which was worn in the immediate vicinity of the apparatus.

Operating Procedure

The vacuum pumps were started and run continuously so as to maintain a constant purge. The boiler-condenser system was considered to be satisfactorily sealed if it could be pumped down to about 100 microns. The desired electrical input was then introduced into the heaters. It took about half an hour for the system to heat up and for the first mercury droplets to start condensing on the nickel tube. The flow of the cooling liquid was then started and adjusted to a value which would yield the desired wall temperature. Slowly the condensation chamber pressure and the various temperatures rose to their steady state values. Data was taken only after complete film condensation was obtained.

Visual Observation of the Condensation Process

Before a run the condenser tube was cleaned with a fine grade of emery paper, buffed, and washed in a running stream of reagent ethyl alcohol.

The condensation initially was in the form of large numbers of very small drops, which because of their size were picked off the surface and carried into the swirling vapor. Slowly the drops would begin to agglomerate with each other, eventually roll downwards, and leave a clean path behind. Small drops would immediately begin to form in this clean trace, and the process would keep on repeating. If sizeable amounts of non-condensable gases were present in the system, the condensation process did not proceed beyond this stage.

With a system well purged of non-condensable gases, the drops would keep on getting bigger, and their contact angle would be seen to decrease. Compared to the initial stages when the drops on the surface were almost complete spheres, they now had hemispherical shapes. Soon the largest drops would begin to leave traces of liquid behind on the track swept by them. These traces would join up to form continuous streams, and these streams in turn would join cross-wise with each other to eventually form a complete film all over the condenser surface.

The whole process of changing over to film condensation usually took a few hours (sometimes as much as ten hours). However, once it was known that the system was being well purged of non-condensable gases, there was never any doubt that film condensation would be eventually obtained. Also, once a film had been obtained, the apparatus could be shut off without any fear of the film immediately breaking up. The next day on starting up, no waiting was necessary to obtain film condensation.

The observation that the condensation remained dropwise and did not change over to a film in the presence of non-condensable gases can

be explained qualitatively. Non-wetting is a direct consequence of the presence of an oxide layer and/or an adsorbed gas layer on the nickel surface. If pure mercury vapor is made to condense on such a surface, it slowly removes these layers, comes into contact with the bare clean metal, and wets it. Recent studies by Umur and Griffith[30] have shown that during dropwise condensation the area between the drops is bare. If, therefore, non-condensable gases (in our case air) are present, they constitute an ever-present source which comes into contact with the condenser surface and can replenish any of the oxide layer removed by the liquid mercury. Hence the condensation does not change over in character. It should be noted that, as is to be expected, once film condensation had been obtained, the introduction of small traces of non-condensables did not cause a reversal to dropwise condensation.

IV. RESULTS AND DISCUSSION

Condensate Film Thickness

The thickness of the mercury condensate film was measured for heat fluxes ranging from 20,000 to 175,000 BTU/hr.ft^2. In every test it was measured at six locations 1/2 in. apart, the highest being 2-1/2 in. from the top of the condenser. The average value of the thickness ranged from 0.0010 in. at the lowest heat flux to 0.0025 in. at the highest.

This average value was assumed to occur at 3-3/4 in. from the top. Assuming further that the thickness follows a 1/4 power law and that there is a linear temperature distribution in the film, a heat transfer coefficient (h_f) can be calculated using the easily derived expression

$$h_f = \frac{4k}{3\delta_1} \cdot \left(\frac{z_1}{L}\right)^{1/4} \tag{10}$$

where δ_1 is the averaged film thickness at a distance z_1 (= 3-3/4 in.), k is the liquid thermal conductivity, and L is the length of the condenser, 6 in.

In Figure 6, h_f is plotted against the film Reynolds number, calculated from the average heat flux using the equation

$$Re_L = \frac{4L}{\mu} \cdot \frac{(q/A)}{\lambda'} \tag{11}$$

The prediction from Nusselt's classical theory (references 7, 8, 9, 10 give the same prediction) is also plotted for comparison. Considering the accuracy of the measurement ($\pm$ 0.00025 in., which is $\pm$ 25% at the

lowest heat flux and $\pm$ 10% at the highest heat flux), the experimental values are in reasonable agreement with the Nusselt prediction. It is important to note that both have magnitudes in the vicinity of 50,000 BTU/hr.ft.^{2} $^\circ$F.

The Condensing Side Heat Transfer Coefficient

Data on the condensing side heat transfer coefficient are presented in Appendix III. These have been obtained for heat fluxes ranging from 35,000 to 150,000 BTU/hr.ft.^{2} and for pressures ranging from 1 to 17 mm. The heat transfer coefficient (h_c) calculated from these measurements had varied from 200 to 4000 BTU/hr.ft.^{2} $^\circ$F and is presented in Table 1. These values are at least an order of magnitude lower than those deduced from the liquid film thickness measurements alone.

All the data were taken with complete film condensation. There were two reasons for doing this: (i) The presence of a film reduced the possibility of having a significant solid-liquid interface resistance. (ii) With mercury vapor molecules colliding and condensing on a liquid mercury interface, the changes of obtaining a reasonably constant value of σ were probably improved. With this same end in view, during the entire period of data taking, the mercury in the system was neither purified in any way nor were any additions made to it.

The general practice followed in taking the data was to vary the wall temperature at certain fixed values of the heat flux, in order to bring out clearly the effect of the pressure on the heat transfer coefficient. The values obtained for a heat flux of 73,200 $\pm$ 1000 BTU/hr.ft.^{2} and with the wall temperature varying from 89 $^\circ$F to 366.5 $^\circ$F (Tests 9-14)

Test No.	Heat Flux q/A (BTU/hr.ft.^{2})	Condenser Wall Temperature T_w (^oF)	Pressure p_v (mm)	Heat Transfer Coefficient on Condensing Side h_c (BTU/hr.ft.^{2} ^oF)	Value of σ Which Fits Theory	Predicted Value Assuming $\sigma = 0.45$ h_{th} (BTU/hr.ft.^{2} ^oF)	$(\frac{h_c - h_{th}}{h_{th}}) \times 100$
1	36,800	64	1.04	188	0.605	170	+ 10.6
2	34,700	183	1.40	386	0.516	358	+ 7.8
3	49,100	63	2.38	209	0.426	214	- 2.3
4	54,700	178	3.22	408	0.381	445	- 8.3
5	53,000	206	3.00	515	0.408	552	- 6.7
6	47,600	329	6.80	2884	0.502	2504	+ 15.3
7	62,100	80	2.90	274	0.442	276	- 0.7
8	61,100	123	2.70	340	0.450	340	+ 0.0
9	72,600	89	3.50	321	0.432	326	- 1.6
10	74,500	262	4.90	1080	0.428	1130	- 4.4
11	74,100	311	6.75	2180	0.473	2120	+ 2.8
12	72,200	331.5	8.40	3080	0.503	2780	+ 10.8
13	73,150	351.5	11.30	3756	0.521	3330	+ 12.8
14	72,500	366.5	14.20	4030	0.487	3820	+ 5.5
15	97,800	98	4.60	425	0.444	430	- 1.2
16	99,400	178	5.00	649	0.430	661	- 1.8
17	101,200	349.5	13.10	3320	0.445	3370	- 1.5
18	99,800	363.5	17.00	3080	0.365	3840	- 19.8
19	127,000	116	5.20	585	0.491	571	+ 2.5
20	127,000	171	5.50	770	0.477	755	+ 2.0
21	146,000	123	7.96	636	0.401	657	- 3.2
22	143,000	180	6.00	893	0.490	866	+ 3.1
23	140,000	191	8.72	839	0.368	915	- 8.3

Table 1

are illustrated in Figure 7. Here as the pressure has increased from 3.50 mm. to 14.20 mm., the condensing heat transfer coefficient has increased from 321 to 4030 BTU/hr.ft.^{2} $^\circ$F.

For each data point equation (7) is applied over the whole length of the condenser, and the value of σ which fits the concept of a liquid-vapor interface resistance is calculated. The validity of the concept is seen from the fact that all the values of σ (almost without exception) lie in the small range 0.45 ± 0.07.

Taking this average value of 0.45, using equation (7) and Nusselt's theory, a theoretical value of the condensing side heat transfer coefficient can be predicted. In Figure 8 the measured and predicted values are compared. The agreement is good with maximum deviations of +15.3% and -19.8%.

It should be emphasized that the small variation in the value of σ is not entirely attributable to experimental error. This is particularly apparent from tests 21, 22, 23. It seems likely that the value of σ, which depends on the state of the liquid surface, is affected by some form of contamination of the experimental system and that the "level of contamination" has varied slightly from test to test. This being the case, too much significance should not be attached to the numerical value of 0.45. Rather, the significant point is that in a system a reasonably constant value is attainable.

The Solid-Liquid Interface

Examination of the condenser tube after a test always revealed the formation of a thin, black coating on the originally shiny nickel surface. This coating was of the order of 0.0001 in. in thickness and

was electrically conducting. It is believed that it was metallic in nature and had a reasonably high thermal conductivity. (Its gamma-ray attenuation was negligible.) It should be noted also that one would not expect its thermal resistance to change with the vapor pressure or with the heat flux. It seems certain, therefore, that the resistance at the solid-liquid interface could not have been a significant factor in lowering the condensing side heat transfer coefficient to values well below the Nusselt predictions.

Non-Condensable Gases

It has already been pointed out in Chapter II that given certain values of the heat flux and the wall temperature, the introduction of non-condensable gases should cause an increase in pressure and a consequent decrease in h_c. That this argument is correct is seen from the data (Appendix III) obtained by introducing small amounts of non-condensable gases into the system. Prior to the introduction of non-condensables, the data of Test 12 was being obtained.

Figure 7 shows clearly how the two effects--one due to a liquid-vapor interface resistance and the other due to non-condensables--act in different ways. Clearly, if a superposing of these two effects were to occur and the quantity of non-condensable gas present were not known, the data obtained could not be properly interpreted.

Data of Previous Investigators

Finally, the question which needs to be answered is whether the trends associated with a liquid-vapor interfacial resistance can be observed in the data of previous investigators.[12,13,14] An

examination of the data reveals that the anticipated trends are not present. The heat transfer coefficients measured at a constant heat flux have not increased with increasing pressure. In the opinion of the authors, a number of separate causes have become superposed on the liquid-vapor interfacial resistance effect in these investigations. As a consequence the presence of the effect has been obscured. These causes are:

(1) A fluctuating value of σ caused either by (i) taking data regardless of the type of condensation occurring, or (ii) unknowingly changing the "level of contamination" in the system.

(2) Possible errors in measurement--this remark is particularly directed to the methods used for measuring the temperatures or their difference directly.

(3) The presence of significant amounts of non-condensable gases.

Data of Misra and Bonilla

Misra and Bonilla's[12] experiments with mercury and sodium have been conducted below atmospheric pressure, and in the light of the interfacial resistance theory, a significant temperature drop at the liquid-vapor interface should have been present in most of their tests. Their data for mercury have been obtained in three different test systems and with all forms of condensation--film, drop, and mixed--occurring on various surfaces. Thus sizeable variations in σ may well have occurred in their tests. In addition, some of the methods used by them for measuring the difference of temperature directly are open to question. Conduction along the leads could have caused serious errors.

Lastly, the experimental evidence given by them to show the absence of non-condensable gases in their equipment is inconclusive. They have plotted the heat transfer coefficient against c.c. of non-condensables per minute passing through the apparatus and extrapolated the resulting curves to intersect the y-axis, assuming that the heat transfer coefficient thus determined was for the case of no non-condensables. This is a very questionable technique because the curves are almost asymptotic with the y-axis. In fact, if the same data points are plotted on a log-log basis (Figure 9), they are seen to lie on straight lines. The important point which needs to be understood is that the rate of leakage (or removal) of non-condensables from a system is not necessarily a measure of the significance of the non-condensable gas. The pertinent quantity is the amount actually present in the system.

Data of Cohn

Cohn[13] has condensed mercury and cadmium inside a long tube, and his apparatus design is such that any non-condensable gas leaking into the condenser tube would be trapped there. He has made no visual observation, but it is likely that dropwise condensation existed. His measured wall temperature may be lower than the actual value because of conduction along the thermocouple wires. This could have produced significant errors since the temperature differences in most of his tests are small. These are small differences between two large measured quantities. He himself recognizes this fact.

He has also condensed steam above atmospheric pressures in the same apparatus. Inspite of the fact that no liquid-vapor interface resistance should have been present with steam at those pressures, he has

obtained dataalong a line having a -1 slope. It seems quite certain, therefore, that the factors mentioned above--presence of non-condensables and temperature measurement error--have been present in his tests with water and have carried over to the liquid metal tests.

Data of Roth

Roth[14] has condensed rubidium on the outside of a tube using air as a coolant. These tests were run at fairly high pressures where significant liquid-vapor interfacial resistance is not expected to be present. Yet his data are the lowest of all the investigators. He makes no mention of attempting to eliminate non-condensable gases and gives no details of his wall temperature measuring technique, stating merely that the thermocouples "were fabricated by drilling a small hole in the tube wall, inserting the thermocouples, and welding them to the wall on the outside." Later he makes the ambiguous statement, "By a cancellation of conduction and radiation errors of these thermocouples, estimates indicate these temperatures are within 3 to 4 percent of each other." That his wall temperature measurement is in error is seen clearly when one uses his data to calculate the heat transfer coefficient on the air side. The air side coefficient seems to vary almost haphazardly with the air flow rate. To some extent this may be due to the variation in the air properties from test to test, but the magnitude of the variation suggests it is due to errors in wall temperature measurement.

Design Recommendation

We conclude from the results of this investigation that the rational design of any condenser, particularly one using liquid metals, requires

that the liquid-vapor interfacial resistance determined from Equation (7), or in some instances Equation (8), must be included in the calculation. In any event, an assumed value of $\sigma = 1.0$ results in a more meaningful upper limit for the predicted heat transfer coefficient than that obtained from the Nusselt theory alone.

V. SUMMARY

Present theories for heat transfer during film condensation of saturated liquid metal vapors take account only of the thermal resistance presented by the condensate film. An examination of previous experimental work shows that a significant thermal resistance additional to that prescribed by current theory must be present. Calculations from kinetic theory indicate that such a resistance can exist at the liquid-vapor interface. For any given fluid and a given heat flux, the interfacial resistance increases with decreasing pressure and with a decreasing value of the condensation coefficient σ (defined as that fraction of all vapor molecules striking the liquid surface which condenses on it).

Experiments have been conducted with mercury vapor condensing on a vertical nickel surface with heat fluxes ranging from 35,000 to 150,000 BTU/hr.sq.ft. Special precautions have been taken to eliminate non-condensable gases. The pressure in the vapor space has varied from 1 mm. to 17 mm. and the measured value of the condensing side heat transfer coefficient from 200 to 4000 BTU/hr.sq.ft.$^{\circ}$F. The increase of the heat transfer coefficient with pressure has been clearly demonstrated. Almost all the data can be fitted to the concept of a liquid-vapor interfacial resistance for values of σ ranging from 0.37 to 0.52.

This scatter in the values of σ is not entirely attributable to experimental error. It seems more likely that the value of σ, which depends on the state of the liquid surface, is affected by some form of contamination of the experimental system.

The thickness of the condensate film has been measured by a gamma-ray attenuation technique, and its thermal resistance is found to be in reasonable agreement with existing theories.

Examination of the solid-liquid interface after a run has revealed the formation of a very thin (approx. 0.0001 in.) electrically conducting, black coating on the originally shiny, polished nickel surface. The thermal resistance of such a coating, which does not come into contact with the vapor, cannot be dependent on the vapor pressure. It is, therefore, considered unlikely that a significant resistance exists at the solid-liquid interface.

Finally, it has been shown that the effect of introducing small traces of non-condensable gases at a given heat flux and condenser wall temperature is to decrease the heat transfer coefficient with increasing pressure.

It is concluded that:

(1) During film condensation of liquid metals, a significant thermal resistance can exist at the liquid-vapor interface.

(2) This resistance is dependent on and increases with decreasing vapor pressure and with a decrease in the value of the coefficient σ.

(3) The coefficient σ, which is a function of the state of the liquid surface, is probably influenced by some form of contamination in the experimental system.

VI. LIST OF SYMBOLS

h	heat transfer coefficient
h_{Nu}	heat transfer coefficient predicted from theories which take account only of the condensate film's thermal resistance
h_{th}	condensing side heat transfer coefficient (predicted by considering liquid-vapor interface resistance)
h_f	heat transfer coefficient deduced from film thickness measurement
h_c	condensing side heat transfer coefficient (measured)
p	pressure
p_s	saturation pressure corresponding to temperature T_s
p_v	pressure of pure saturated vapor in bulk space
T	temperature
T_w	condenser wall temperature at outer surface
T_s	temperature of liquid at liquid-vapor interface
T_v	saturation temperature corresponding to pressure p_v
ΔT_f	temperature drop across condensate film
ρ	density
ρ_l	liquid density
ρ_v	density of saturated vapor at conditions p_v and T_v
k	liquid thermal conductivity
λ	latent heat of vaporization
λ'	equivalent latent heat
μ	liquid viscosity

ν	liquid kinematic viscosity
C_p	liquid specific heat
Pr	Prandtl number
m	mass of a molecule
M	molecular weight
σ	condensation coefficient
N/A	flux of molecules (number/unit time - unit area)
w/A	mass flux (mass/unit time - unit area)
q/A	average heat flux (units of heat/unit time - unit area)
ϕ	non-dimensional number - a measure of bulk movement of vapor molecules towards interface - Equation (5)
Γ	non-dimensional correction factor - Equation (4)
z	distance along condenser
δ_1	averaged film thickness measurement
L	length of condenser
Re_L	film Reynolds number at z = L
g	acceleration due to gravity
$\bar{R}$	universal gas constant

VII. REFERENCES

1. Nusselt, W., Zeitsch. d. Ver. deutsch. Ing., 60, 541, (1916)
2. Seban, R. A., Trans. ASME, 76, 299, (1954)
3. Bromley, L. A., Ind. and Eng. Chem., 44, 2966, (1952)
4. Rohsenow, W. M., Trans. ASME, 78, 1645, (1956)
5. Sparrow, E. M. and Gregg, J. L., Trans. ASME, Series C, 81, 13, (1959)
6. Mabuchi, I., Trans. Japan Soc. Mech. Engrs., 26, 1134, (1960)
7. Chen, M. M., Trans. ASME, Series C, 83, 48, (1961)
8. Koh, C. Y., Sparrow, E. M., and Hartnett, J. P., Int. J. Heat and Mass Transfer, 2, 69, (1961)
9. Koh, C. Y., Trans. ASME, Series C, 83, 359, (1961)
10. Chato, J. C., ASHRAE Journal, 4 (2), 52, (1962)
11. McAdams, W. H., "Heat Transmission," McGraw Hill
12. Misra, B. and Bonilla, C. F., Chem. Eng. Prog. Sym., Series No. 18, 52, 7, (1956)
13. Cohn, P. D., M. S. Thesis, Oregon State College, (1960)
14. Roth, J. A., Report ASD-TDR-62-738, Wright-Patterson AFB, (1962)
15. General Electric Co., Missile and Space Div., Cincinnati, "Alkali Metals Boiling and Condensing Investigations," Proceedings of 1962 High Temperature Liquid Metal Heat Transfer Technology Meeting held at Brookhaven National Lab
16. General Electric Co., Qtr. Report 1, Ctr. NAS 5-681, Sept. 1962
17. Broglio, L., Ravelli, G., and Buongiorno, C., Report No. 59, Sch. of Aeronautical Engineering, Univ. of Rome, (1961)
18. Dukler, A. E., Chem. Eng. Progr. Sym. Series No. 30, 56, 1, (1960)
19. Lee, J. H., A. F. Materials Lab., Wright-Patterson AFB, (1963)

20. Schrage, R. W., "A Theoretical Study of Interphase Mass Transfer," Columbia University Press, New York, (1953)

21. Silver, R. S. and Simpson, H. C., "The Condensation of Superheated Steam," Proceedings of a conference held at the National Engineering Lab., Glasgow, (1961)

22. Sukhatme, S. P. and Rohsenow, W. M., Report presented at Third Annual Liquid Metal Heat Transfer Technology Meeting held at Oakridge National Lab., Sept. 1963

23. Hertz, H., Ann. Phys. Lpz., 17, 177, (1882)

24. Knudsen, M., Ann. Phys. Lpz., 29, 179, (1909)

25. Knudsen, M., Ann. Phys. Lpz., 47, 697, (1915)

26. Volmer, M. and Estermann, J., Z. Physik, 7, 1, (1921)

27. Paul, B., ARS Journal, 32, 1321, (1962)

28. Silver, R. S., Engineering, 161, 505, (1946)

29. Kirillov, P. L., Subbotin, V. I., Suvorov, M. Ya., and Troyanov, M. F., J. Nucl. Energy, Part B: Reactor Technology 1, 123, (1959)

30. Umur, A. and Griffith, P., "Mechanism of Dropwise Condensation," Report 9041-25, Dept. of Mechanical Eng., M.I.T., May 1963

31. Jeffrey, J. O., Cornell Univ. Engineering Experiment Station, Bulletin No. 21, (1936)

32. Webber, J. H., S. M. Thesis, Course II, M.I.T., (1955)

33. MacLeod, A. A., Doctor of Science Thesis, Carnegie Tech., (1951)

34. Belkin, H. M., Doctoral dissertation, Carnegie Tech., (1953)

35. Dukler, A. E. and Bergelin, O. P., Chem. Eng. Prog., 48, 557, (1952)

36. Hooker, H. H. and Popper, G. F., Argonne National Lab., Report ANL-5766, (1958)

37. Richardson, B. L., Argonne National Lab., Report ANL-5949, (1958)

38. Christensen, H., Ph.D. Thesis in Nuclear Engineering, M.I.T., (1961)

APPENDIX I

CONDENSER WALL TEMPERATURE MEASUREMENT

The average temperature of the condenser wall was determined by making a precise measurement of the electrical resistance of a section of the condenser tube. This temperature was desired to an accuracy of $\pm$ 1 ^{o}F. Although a thermocouple can give this accuracy easily in a large space, it is difficult to locate a thermocouple accurately in a thin wall and to prevent errors due to conduction along the leads. Also, a thermocouple reads a local temperature and upsets the heat flux lines in the very region of its measurement. All these considerations led to the idea of using the condenser tube itself as a "resistance thermometer."

Principle of Method

The "resistance thermometer" technique depends on the observation that the electrical resistance of metals increases with temperature. The resistance R of a metal block of length l and cross-section area A is given by

$$R = \frac{Sl}{A} \tag{12}$$

where S is called the resistivity of the metal.

Essentially, the change in resistance with temperature is due to a change in the resistivity and not a change in the dimensions. Over short ranges of temperature, the resistivity generally increases

linearly with temperature so that we may express equation (12) in the form

$$R = \frac{S_o [1 + \alpha (T - T_o)] l}{A} \qquad (13)$$

where S_o is the resistivity at some reference temperature T_o, and α, the constant of linearity, is called the temperature coefficient of resistance. Thus over short ranges of temperature, the change of resistance with temperature is also approximately linear.

The feasibility of using this method depends on the ability to measure the low resistance of metal tubes. The desired accuracy would depend on the accuracy to which the temperature is required.

A detailed analysis is given by Jeffrey,[31] and his paper has formed the basis for designing the present set-up. The method has the inherent advantage of averaging out temperature variations along the length and circumference of the condenser tube. Also, for a thin-walled condenser in which the temperature gradient is very close to being linear, Jeffrey has shown that even for work of the highest precision, the temperature corresponding to the measured resistance may be taken to be equal to the average of the temperatures at the outer and inner surface of the condenser.

Description of Set-up

The choice of Nickel 200 among all other types of nickel was based on the consideration that given a certain set of dimensions, it was desirable to obtain the maximum possible change in resistance for every

degree change in temperature. It was estimated that a 1 inch length of a Ni 200 condenser tube, 3/4 in. diameter, and 0.032 in. wall thickness would have a resistance of about 50 $\mu\Omega$ (micro-ohms) at 32 ^{o}F and change in resistance by 0.15 $\mu\Omega$ for every ^{o}F change in temperature.

It takes about three diameters (2-1/4 in.) from the point of introduction of the electric current before the flow lines become parallel to each other. The condenser tube was 6 in. long, and hence the maximum possible length over which the resistance could be measured was 1-1/2 in. Since the temperature was desired to an accuracy of $\pm$ 1 ^{o}F, the resistance of the order of 100 $\mu\Omega$ was required to an accuracy of $\pm$ 0.2 $\mu\Omega$.

The resistance was measured by the "potentiometer method." In this method the unknown resistance is connected in series with a standard resistance. A current is passed through both of them, and the potential drop across both is measured. The ratio of the potential drops is a measure of the unknown resistance. The magnitude of the current passed is determined by the following considerations:

(i) The larger the current, the harder it is to maintain it at a constant value. The accuracy of the method depends largely on the proposition that the current stays at a constant value while the two potential drops are being measured.

(ii) The current must be of such a value that the heat generated in the tube by its passage is negligible compared to that passing through the condenser wall during an actual test. Calculations indicated that to satisfy this condition the current had to be less than 20 amps.

(iii) The current must be of at least such a magnitude that the change in potential drop due to a change of 0.2 $\mu\Omega$ in the unknown resistance should be easily measured on the potentiometer. From this consideration it was desirable to have a current of at least 5 amps.

As a compromise a value of approximately 10 amps was used. The current was supplied by a 2.1 volt Willard battery with a capacity of 600 amp.-hours. A carbon compression rheostat helped to regulate the current. The standard resistance was a Leeds and Northrup 0.001 ohm precision resistor having a limit of error of $\pm$ 0.04%. In actual use the current was found to drop at a slow, steady rate. The method adopted, therefore, was to alternately measure the potential drop across the known and unknown resistance at equal intervals of time. Interpolation on one set yielded values at the same instants of time.

The set-up is sketched in Figure 10. A copper ring was soldered near the top of the condenser tube, and one current terminal was attached to it. The other current lead (14 gage Ni wire) was fusion welded to the bottom of the condenser tube on the inside. The potential leads made of 20 gage Ni wire were also fusion welded to the condenser wall. All leads were insulated with teflon tubing.

The nickel potential leads coming out of the condenser were soldered to copper leads and the junctions placed in an ice bath to prevent the generation of a thermo-electric e.m.f. Since there were no dissimilar metals anywhere else in the circuit, no thermo-electric e.m.f. should have been generated. In practice a small e.m.f. was always detected, and it is suspected that it was generated at the junctions of the nickel

wires and the condenser tube due to dissimilarities in composition and due to a small temperature variation along the tube length. The practice followed was to measure this thermo-electric e.m.f. and to correct the measured potential drop for it. In addition, the current through the tube was reversed so that the thermo-electric e.m.f. correction was also reversed in sign. A measurement of the unknown resistance was considered satisfactory only when the values obtained with the current flowing in either direction agreed within certain limits determined by the conditions of the particular test.

Calibration

The condenser was calibrated at the melting point of ice, at a steady room temperature, at the boiling point of water, and at three higher temperatures inside a furnace. The calibration curve is shown in Figure 11. Due to polishing and buffing of the surface between runs and a consequent decrease in the cross-sectional area, there was a gradual increase in the resistance. The procedure followed after every few runs was to re-calibrate the tube at one or two temperatures and to scale the whole calibration curve up.

Mercury Film Correction

Since the mercury condensed as a film on the condenser surface, it was necessary to correct for the fact that the measured resistance during a test was the sum of two resistances in parallel--one due to the nickel tube and the other due to the mercury film. Luckily mercury has a resistivity about ten times that of nickel, and in addition, its film thickness was never more than one-tenth that of the tube. Its

resistance, therefore, was always at least two orders of magnitude greater than the nickel, and a precise correction was possible.

APPENDIX II

CONDENSATE FILM THICKNESS MEASUREMENT

A number of methods for measuring film thicknesses have been used by previous investigators, and they were all considered before a gamma-ray attenuation method was selected. Calculations indicated that if present theories were valid, a maximum film thickness of 0.003 in. was to be expected. An accuracy of $\pm$ 0.00025 in. seemed desirable.

Webber[32] has used a pointer mounted on a micrometer to measure thicknesses of water films. The difference between the readings obtained by contact with the metal surface and with the film surface is the film thickness. The main shortcoming of the method is that since ripples form on the surface, the probe makes contact first with the top of the waves, and the thickness to the crest is measured. Also, an effective sliding seal for the probe is required in the walls of the condensation chamber. MacLeod[33] and Belkin[34] have used high speed photography. Photographs are taken of a certain length of the condenser tube with and without condensation. These are enlarged and the areas measured by a planimeter. Belkin states that the average error in his measurements is 0.001 in. Dukler and Bergelin[35] have used a capacitance method which yields an accuracy of about 0.001 in.

In contrast to all these methods, a gamma-ray attenuation technique can yield the desired accuracy if a suitable radio-active source, which is particularly sensitive to small thickness variations in mercury, can be found and if calculations show that a source of prohibitive strength

is not required. Inherent in the method are the advantages that the film is not touched while making the measurement and that the entire measuring device can be placed outside the condensing chamber. It is merely necessary to beam the gamma rays in the right direction.

Theory

If mono-energetic gamma radiation of intensity I_o is beamed through a material, a part of it is absorbed through one of three processes: (i) photo-electric effect (ii) pair production (iii) Compton scattering effect. The reduced intensity leaving the material is related to the entering value by the relation

$$I = I_o e^{-\mu d} \tag{14}$$

where d is the thickness of the material and μ is the total linear absorption coefficient of the material for the particular energy.

The Radio-active Source

Much of the information needed for the design of the various components was obtained from the work done at the Argonne National Laboratory by Hooker and Popper,[36] Richardson,[37] and Christensen.[38] A plan view of the set-up is shown in Figure 12. In addition to the mercury film, the gamma rays had to penetrate through the walls of the condensing chamber made of stainless steel, the condenser tube made of nickel, and the cooling fluid. These auxiliary thicknesses were about two orders of magnitude bigger than the mercury film. It was necessary, therefore, that the radio-active source to be used should have an energy spectrum

maximum in a region where mercury's absorption coefficient far exceeds that of stainless steel, nickel, and water. A readily available source which satisfies this requirement is Co^{57}. It has a maximum in its energy spectrum at 120 kev and a half-life of 270 days. Mercury has a K edge at 82 kev, and in the range 100 to 200 kev, its absorption coefficient is about 25 times that for steel and nickel and 150 times that for water.

The strength of the Co^{57} source was determined by the following considerations:

(i) Since the condensation was taking place on a tube, the gamma-ray beam had to be as narrow as possible. For the 3/4 in. dia. condenser tube used, calculations indicated that the beam could be upto 1/4 in. in diameter.

(ii) The count rate (with the background subtracted) obtained with the maximum film thickness had to be at least of the order of the background count.

(iii) The counts obtained in a reasonable period of time for two different film thicknesses only 0.00025 in. apart had to be separated by an amount which exceeded the possible count variation due to statistical fluctuations in the gamma-ray emission from the source.

With these factors in mind a 2 mc source was used.

The source was received in liquid form. It was dried and sealed in a plexiglass vial and placed inside a cylindrical lead container (Figure 13). While making a measurement only the cover was removed.

Instrumentation

The radio-active source was mounted on a horse-shoe shaped plate which fitted around the circular walls of the jacket surrounding the

condensing chamber. The plate could be traversed vertically so that the film thickness at various points along the condenser length could be determined. A scintillation counter (Model 10-8) with a 1 in. dia., 1/2 in. thick Thallium activated Sodium Iodide crystal fitted on was fixed to the traversing plate in line with the gamma-ray source and diametrically opposite from it. The scintillation counter consisted of a photo-multiplier tube and a pre-amplifier. The photo-tube was fed from a High Voltage Power supply (500-1360 V; Model 40-8B). The output of the pre-amplifier was fed into an amplifier-discriminator (Model 30-19) before being counted on a seven decade electro-mechanical scalar (Model 49-30). All the instruments were obtained from the Radiation Instrument Development Laboratory.

Lead shielding was provided around the crystal and photo-tube to cut down the background count. The gamma radiation entered through a 3/8 in. diameter hole drilled in the shielding in line with the beam. Suitable precautions were taken to obtain proper alignment of the source and crystal with the condenser tube. All safety measures required by the Radiation Protection Office were scrupulously observed.

Calibration

The radio-active source was calibrated by inserting thin mercury films of known thickness in the path of the gamma rays. The films were obtained by pressing mercury between two plexiglass plates separated a known distance by thickness gages. The plexiglass plates themselves absorb a small amount of radiation, and suitable account was taken of that fact. It is important to realize that since the source is not

mono-energetic, the variation in count with the mercury's thickness is dependent on the thicknesses of the other materials even though they remain constant.

The calibration obtained is plotted in Figure 14. Since the gamma rays passed through two film thicknesses during an actual test, the value obtained from Figure 14 has to be halved. The calibration should remain unchanged although the source decays, because the ratio of the count obtained with a certain film thickness to that obtained with no film thickness is plotted on the y-axis. This fact was checked experimentally. Before a run on any particular day, it was only necessary to obtain the count with no mercury film in order to use the calibration plot. The source decay during a period of 24 hours was negligible.

There were two differences which distinguished what happened during an actual test from the calibration state.

(i) During the calibration the gamma rays when not penetrating through any of the solids or liquids in its path passed through air. During an actual test, on the other hand, they passed through mercury vapor instead of air for part of the distance. It was checked that the difference in attenuation caused by the mercury vapor as compared to air was negligible.

(ii) The mercury film squeezed between plates during the calibration was a smooth film of uniform thickness in contrast to the film condensing on the nickel tube which had ripples on it. If the ripples had caused deep troughs and high crests, there was no assurance that the thickness picked up from the scintillation counting was a measure of the average thickness since the

relationship between the count rate and the film thickness was exponential and not linear. Visual observations, however, indicated that although a certain amount of waviness was present, the amplitude of the waves was quite small.

Counting Procedures

The counting was done for a period of five minutes and always repeated once. The film thickness during any particular test was measured at distances 2-1/2, 3, 3-1/2, 4, 4-1/2, and 5 in. from the top of the condenser. The maximum and minimum values of thickness measured over the whole series of tests were 0.0025 in. and 0.0005 in. Almost without exception during a particular test at any particular spot, the measurement did not vary by more than 0.00025 in. Along the length of the condenser, however, variations of the order of 0.0005 in. occurred frequently. These were attributed to the following causes:

(i) There was some swirl in the flow rather than a purely normal flow towards the condensing surface.

(ii) Since the entire condenser surface was not visible, small patches in the invisible portion sometimes remained unwetted and caused higher count rates.

Occasionally a few drops of mercury would be thrown onto the walls of the condensing chamber. They would intercept the gamma rays and lower the count rate. If an unusually high thickness was measured, it was attributed to this cause and was discarded.

It will be noted that although sources of error in the measurement technique are discussed in this section, no mention is made of errors arising from the electronics of the system. The measuring instruments were purchased as one unit, and we have relied on the specifications given by the supplier. Care has been taken not to expose certain components to temperature fluctuations.

APPENDIX III

DATA

1. Condenser:

Material - Nickel 200

Length 6 in.; O.D. 0.750 in.; I.D. 0.686 in.

Inner Tube O.D. 0.500 in.; I.D. 0.375 in.

Temperature drop of condenser wall = 1 ^{o}F for a heat flux of 25,000 BTU/hr.ft.^{2} ^{o}F

2. Cooling Fluids:

(i) Water

(ii) Dow Corning 200 silicone oil (2 centistokes)

Specific gravity 0.873;

Thermal conductivity at 77 ^{o}F = 0.0629 BTU/hr.ft.^{o}F

Boiling point 446 ^{o}F at 760 mm. (?)

Specific heat Cp (BTU/lbm.^{o}F) = $0.417 + 2.34 \times 10^{-4}$ (T ^{o}F - 32)

3. Column (1) Test Number

(2) Date of Test

(3) Coolant - W for water; S for silicone oil

(4) Coolant flow rate - lbm/min.

(5) Rise of temperature of cooling fluid - ^{o}F

(6) Average wall temperature - ^{o}F

(7) Temperature in vapor space - ^{o}F

(8) Pressure in vapor space - mm. of mercury

(9) Inlet temperature of coolant - ^{o}F

(1)	(2)	(3)	(4)	(5)	(6)	(7)	(8)	(9)
1	2-2-64	W	24.00	2.51	62	281	1.04	39.5
2	2-2-64	W	0.80	70.90	181	290	1.40	54
3	2-14-64	W	26.20	3.07	61	322	2.38	39
4	2-2-64	W	1.58	56.50	176	331	3.22	-
5	2-15-64	W	0.72	120.10	204	328	3.00	48
6	2-15-64	S	7.26	24.90	327	350	6.80	70
7	2-2-64	W	22.40	4.54	77	327	2.90	39
8	12-14-64	W	9.38	10.70	120	321	2.70	43
9	2-14-64	W	26.06	4.55	86	348	3.50	39
10	2-5-64	S	25.00	11.30	259	345	4.90	93
11	2-5-64	S	18.12	15.55	308	358	6.75	93
12	2-6-64	S	16.60	16.50	328.5	367	8.40	86
13	2-5-64	S	11.92	22.80	348.5	380	11.30	92
14	2-5-64	S	5.45	49.40	363.5	392	14.20	89
15	2-2-64	W	22.00	7.27	94	349	4.60	-
16	2-2-64	W	3.88	42.00	174	352	5.00	43
17	2-6-64	S	24.90	15.43	345.5	392	13.10	100.5
18	2-6-64	S	22.30	16.96	359.5	400	17.00	97
19	2-14-64	W	25.70	8.06	111	368	5.20	39
20	2-14-64	W	8.00	25.90	166	-	5.50	40
21	2-2-64	W	25.90	9.20	117	384	7.96	39
22	12-14-64	W	9.84	23.80	174	367	6.00	43
23	2-2-64	W	4.84	47.20	185	388	8.72	-
Effect of non-condensables on data of Test No. 12:								
24	2-6-64	S	16.60	17.40	334.5	389	13.00	91
25	2-6-64	S	16.60	17.19	331	394	15.80	87

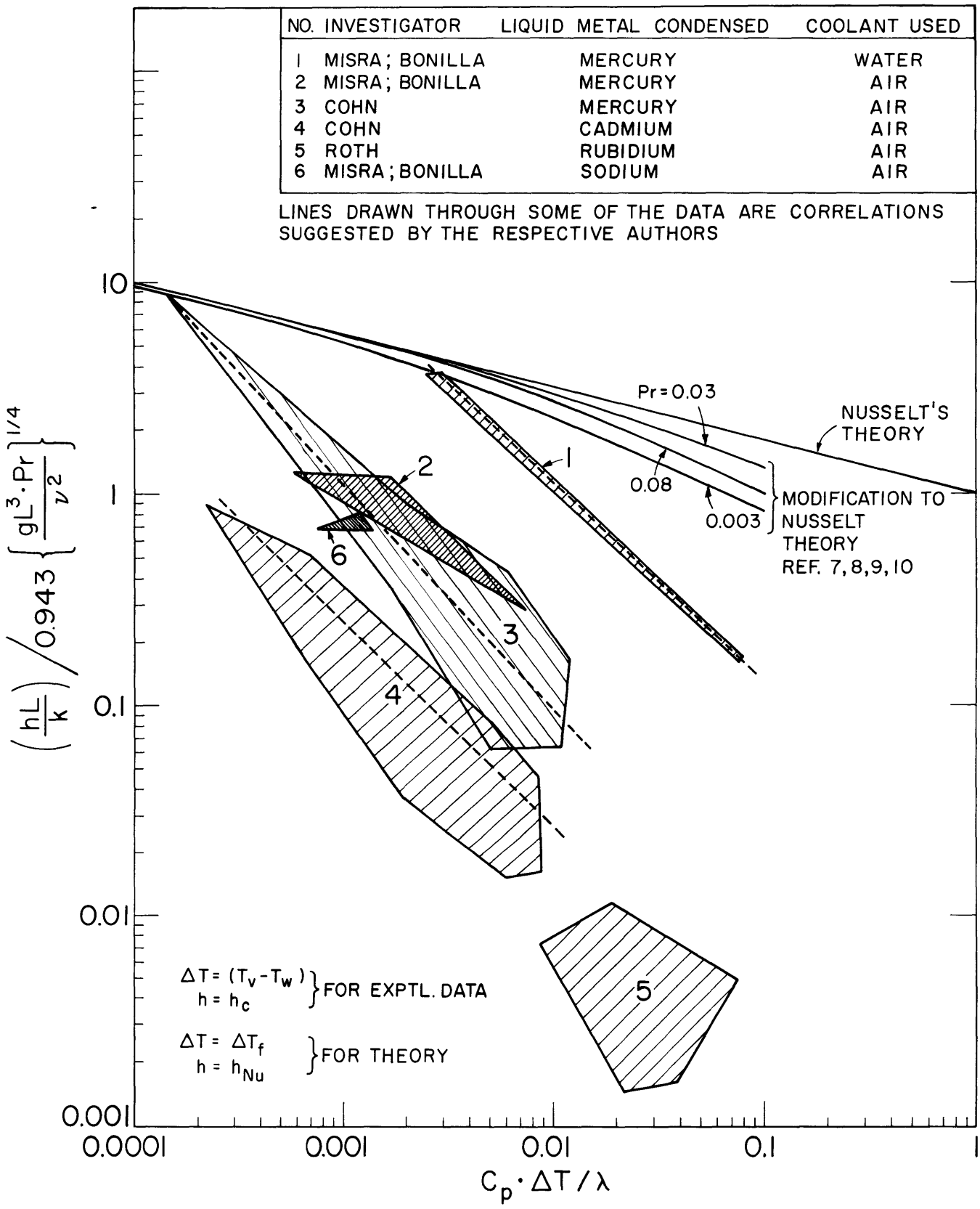

FIG. 1 COMPARISON OF EXISTING THEORIES WITH AVAILABLE DATA

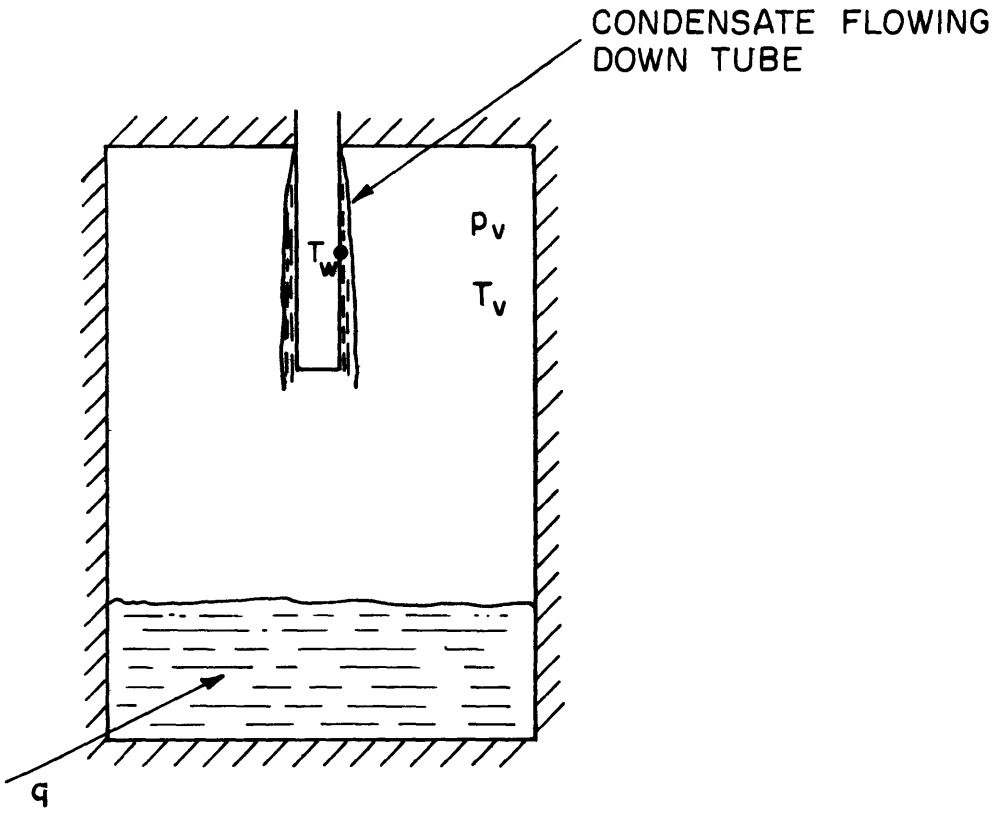

FIGURE 2

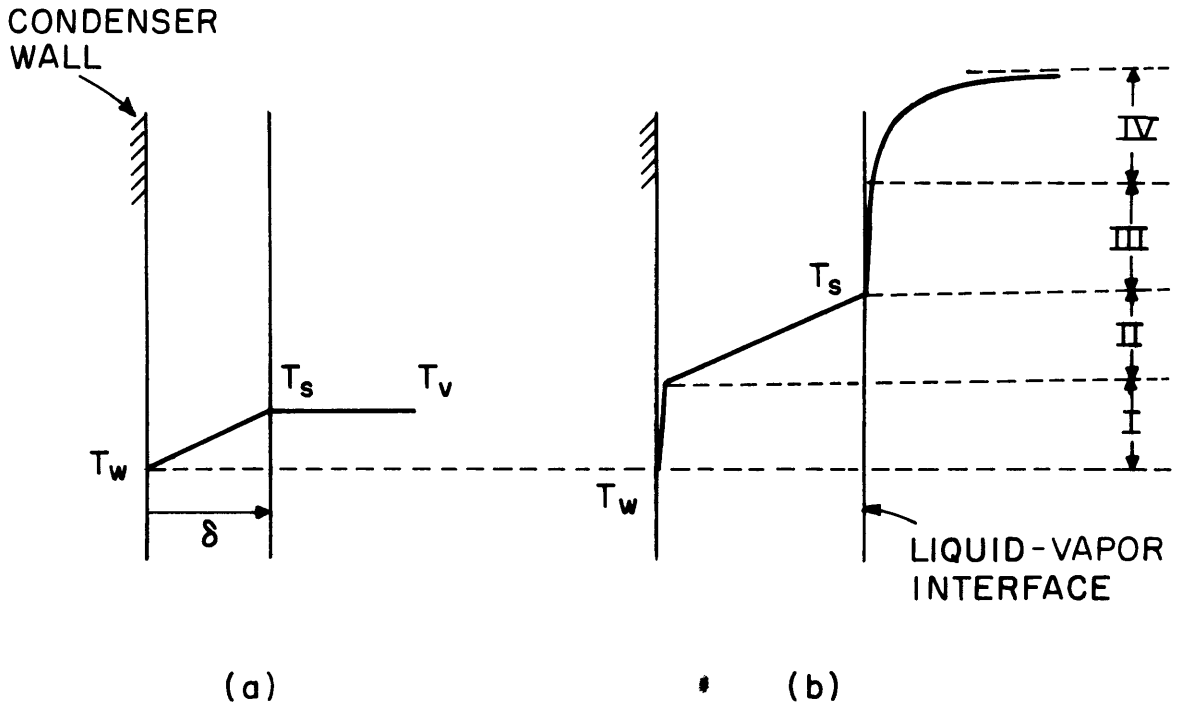

TEMPERATURE DROPS

- I : AT SOLID-LIQUID INTERFACE
- II : ACROSS CONDENSATE FILM
- III : AT LIQUID-VAPOR INTERFACE
- IV : DUE TO PRESENCE OF NON-CONDENSABLES

FIGURE 3

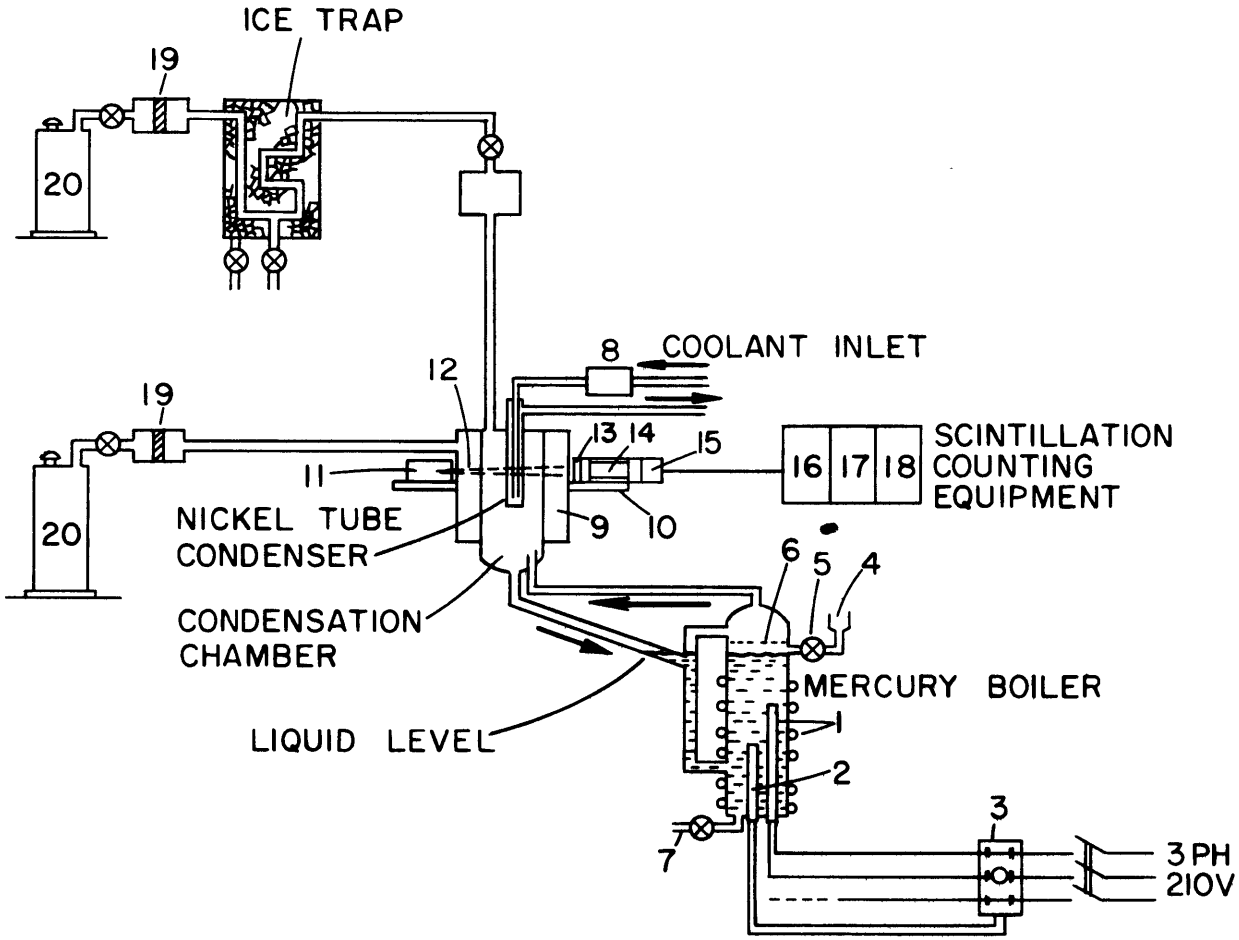

1. ELECTRIC HEATERS
2. THERMAL CUT-OUT SWITCH
3. MAGNETIC CONTACTOR
4. MERCURY FILLING CUP
5. VALVE
6. WIRE MESH SCREEN
7. MERCURY DRAIN LINE
8. FLOWMETER
9. JACKET
10. VERTICALLY TRAVERSING PLATE
11. RADIOACTIVE SOURCE HOLDER
12. GAMMA RAYS
13. SCINTILLATION CRYSTAL
14. PHOTO TUBE
15. PRE-AMPLIFIER
16. HIGH VOLTAGE UNIT
17. AMPLIFIER
18. SCALAR
19. MERCURY VAPOR ABSORBER
20. VACUUM PUMP

FIGURE 4 SCHEMATIC DIAGRAM OF APPARATUS

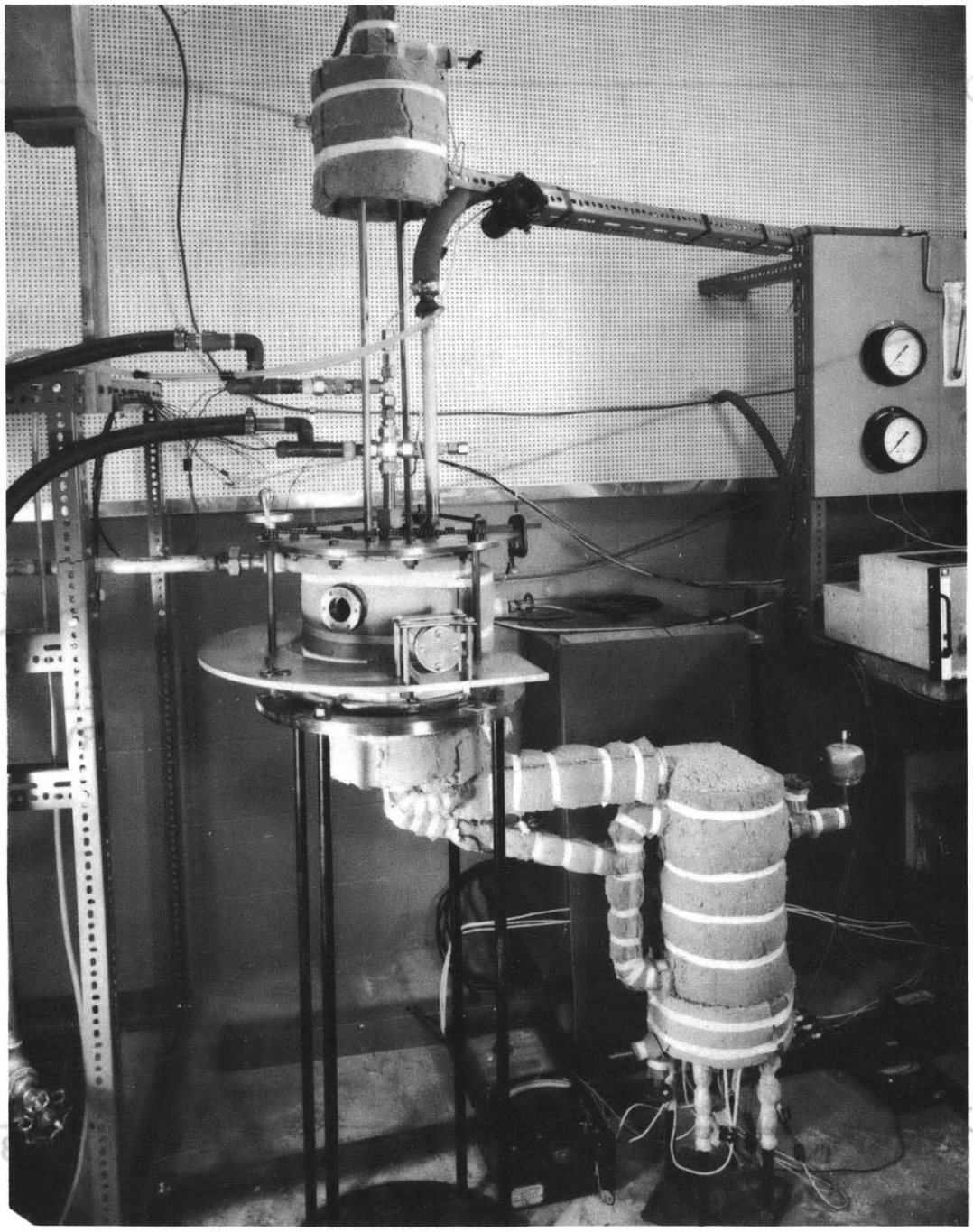

Fig. 5 Photograph of Apparatus (Insulation partially removed)

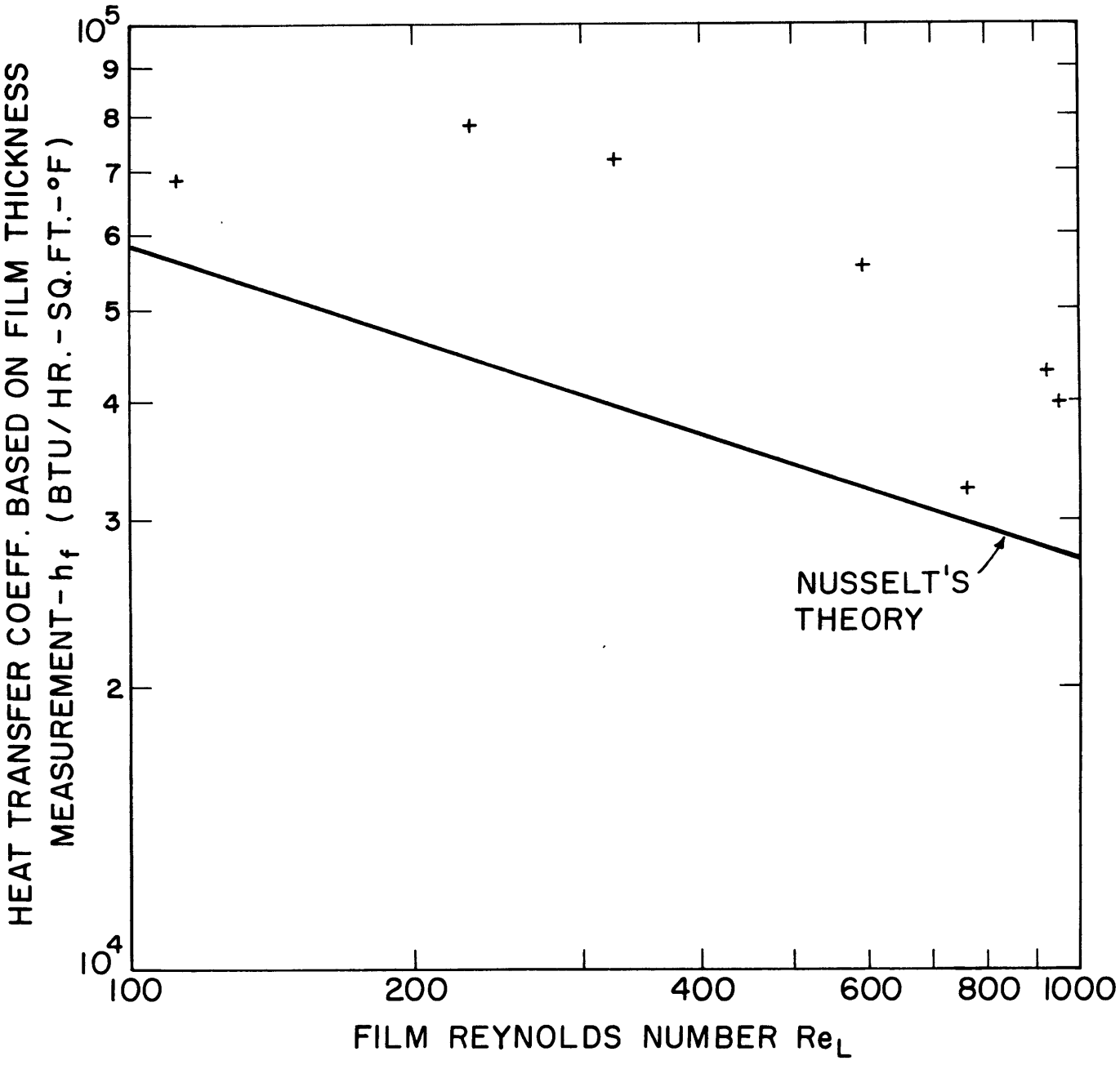

FIG.6 COMPARISON BETWEEN NUSSELT THEORY AND HEAT TRANSFER COEFFICIENT BASED ON FILM THICKNESS MEASUREMENT

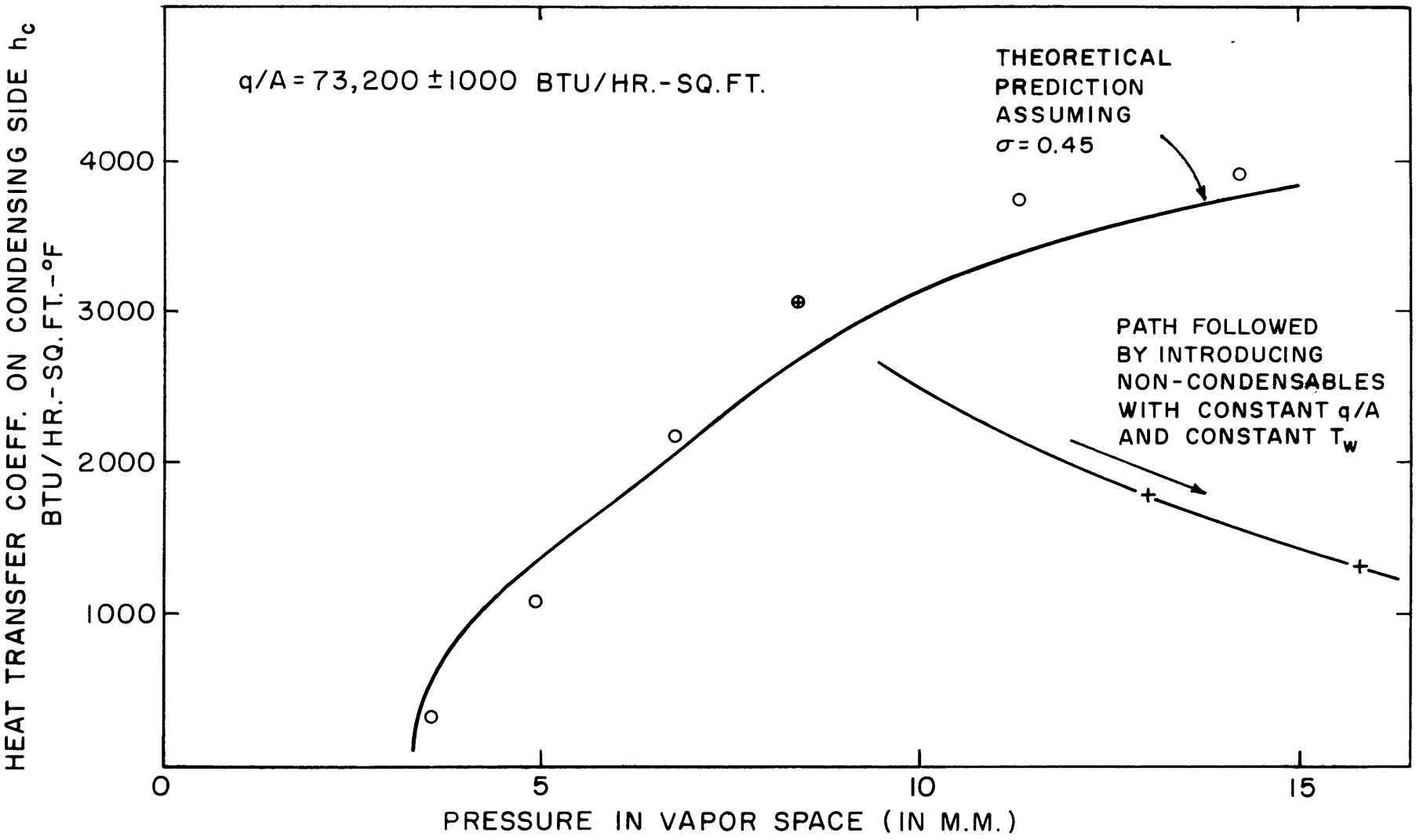

FIG. 7 VARIATION OF HEAT TRANSFER COEFFICIENT WITH PRESSURE (CONSTANT HEAT FLUX)

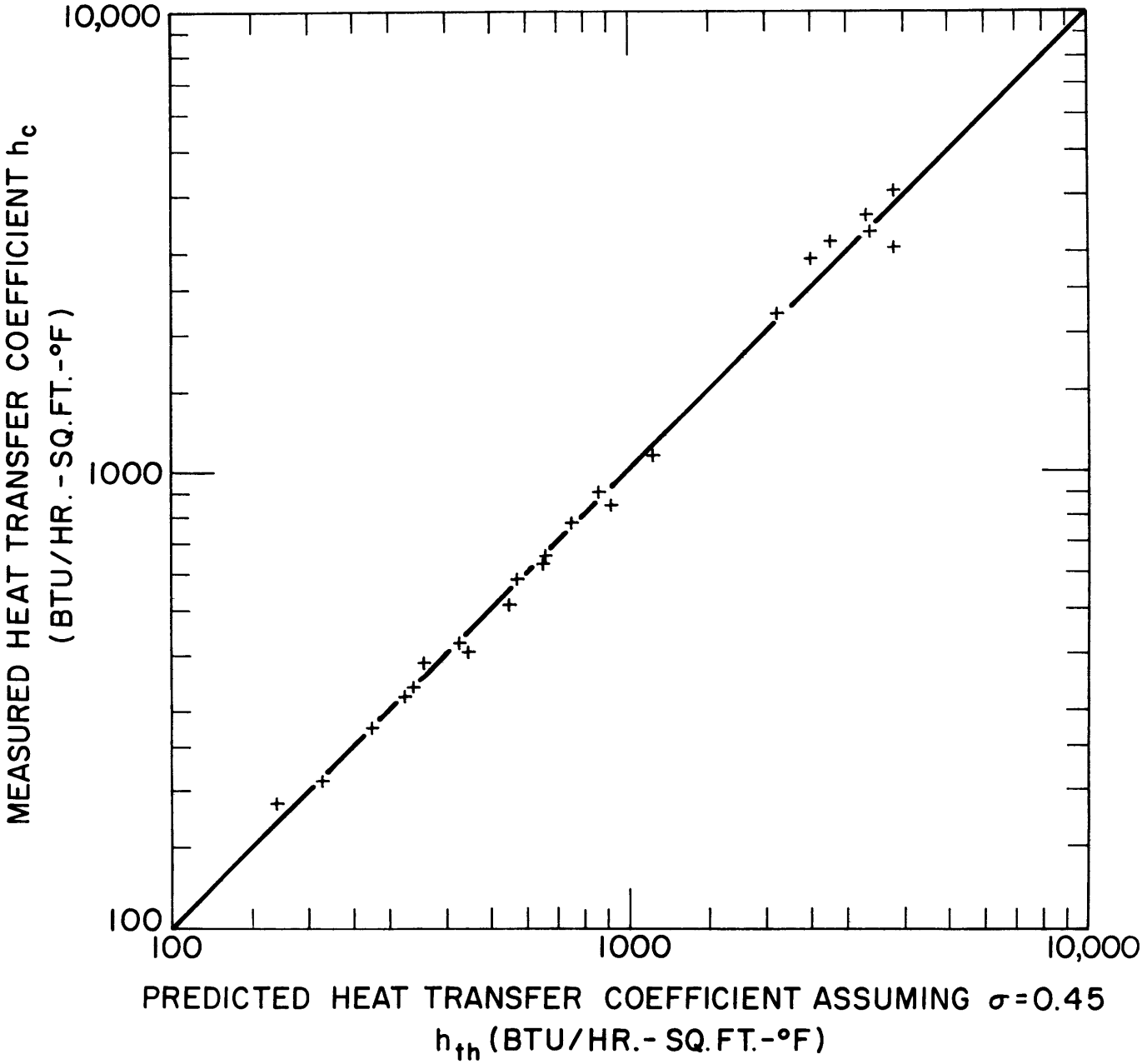
10,000
1000
100
100
1000
10,000
MEASURED HEAT TRANSFER COEFFICIENT h_c
(BTU/HR.-SQ.FT.-°F)
PREDICTED HEAT TRANSFER COEFFICIENT ASSUMING $\sigma = 0.45$
h_{th} (BTU/HR.-SQ.FT.-°F)

FIGURE 8

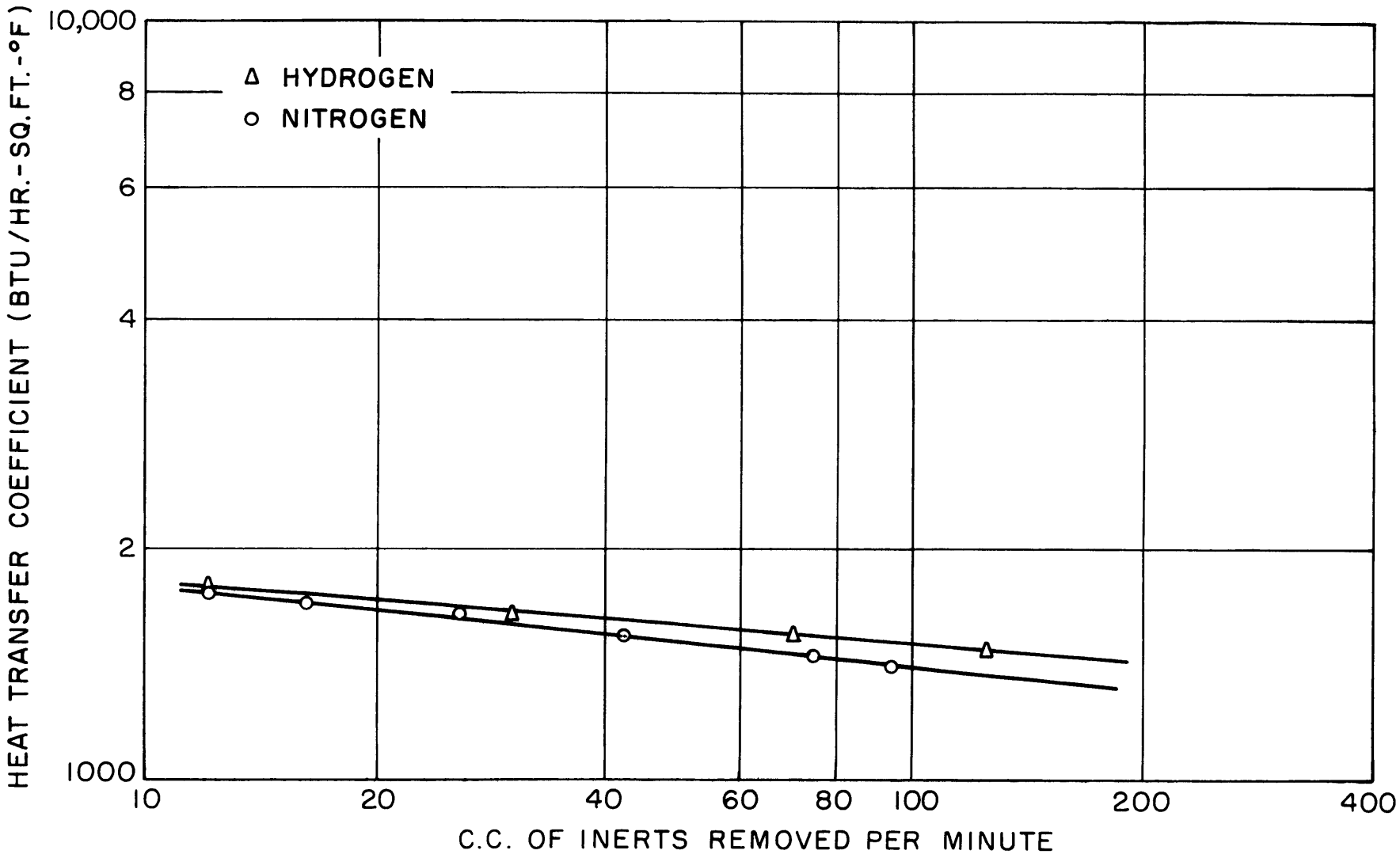

FIG. 9 MISRA AND BONILLA DATA FOR NON-CONDENSABLES — REPLOTTED ON LOG-LOG BASIS

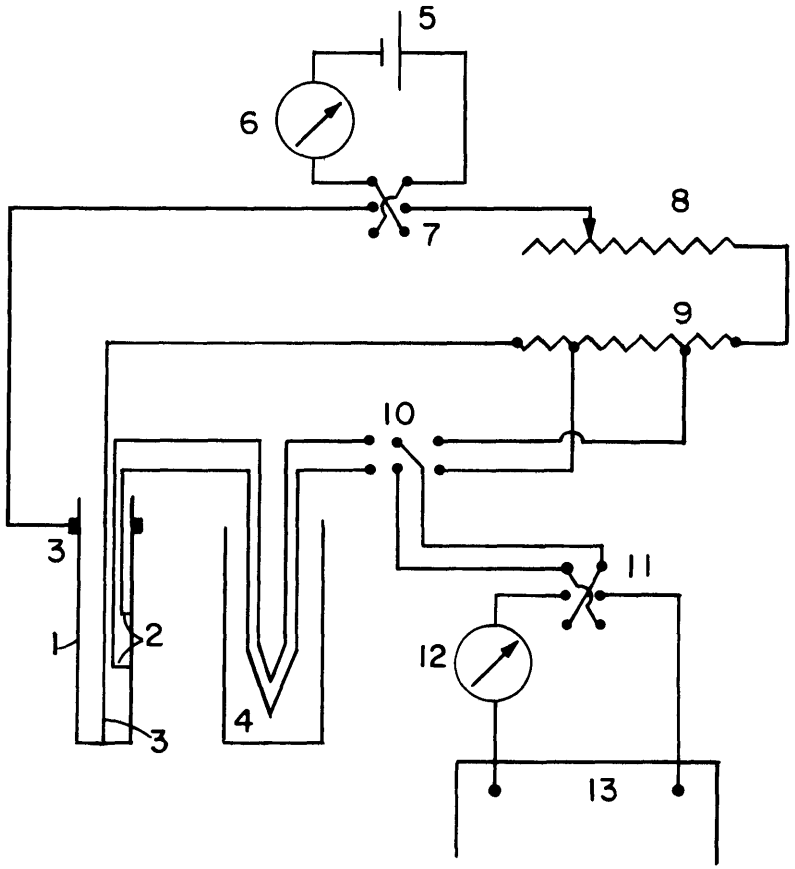

1. NICKEL CONDENSER TUBE
2. 20 GAGE NI WIRES FUSION WELDED TO TUBE WALL
3. CURRENT LEADS
4. NI-CU JUNCTIONS IN ICE BATH
5. 2.1 VOLT WILLARD BATTERY
6. D.C. AMMETER 0-20 AMPS.
7. CURRENT REVERSING SWITCH
8. CARBON COMPRESSION RHEOSTAT
9. 0.001 Ω PRECISION RESISTOR
10. SWITCH
11. REVERSING SWITCH
12. GALVANOMETER
13. RUBICON POTENTIOMETER

FIGURE 10 CIRCUIT FOR MEASURING ELECTRICAL RESISTANCE OF CONDENSER TUBE.

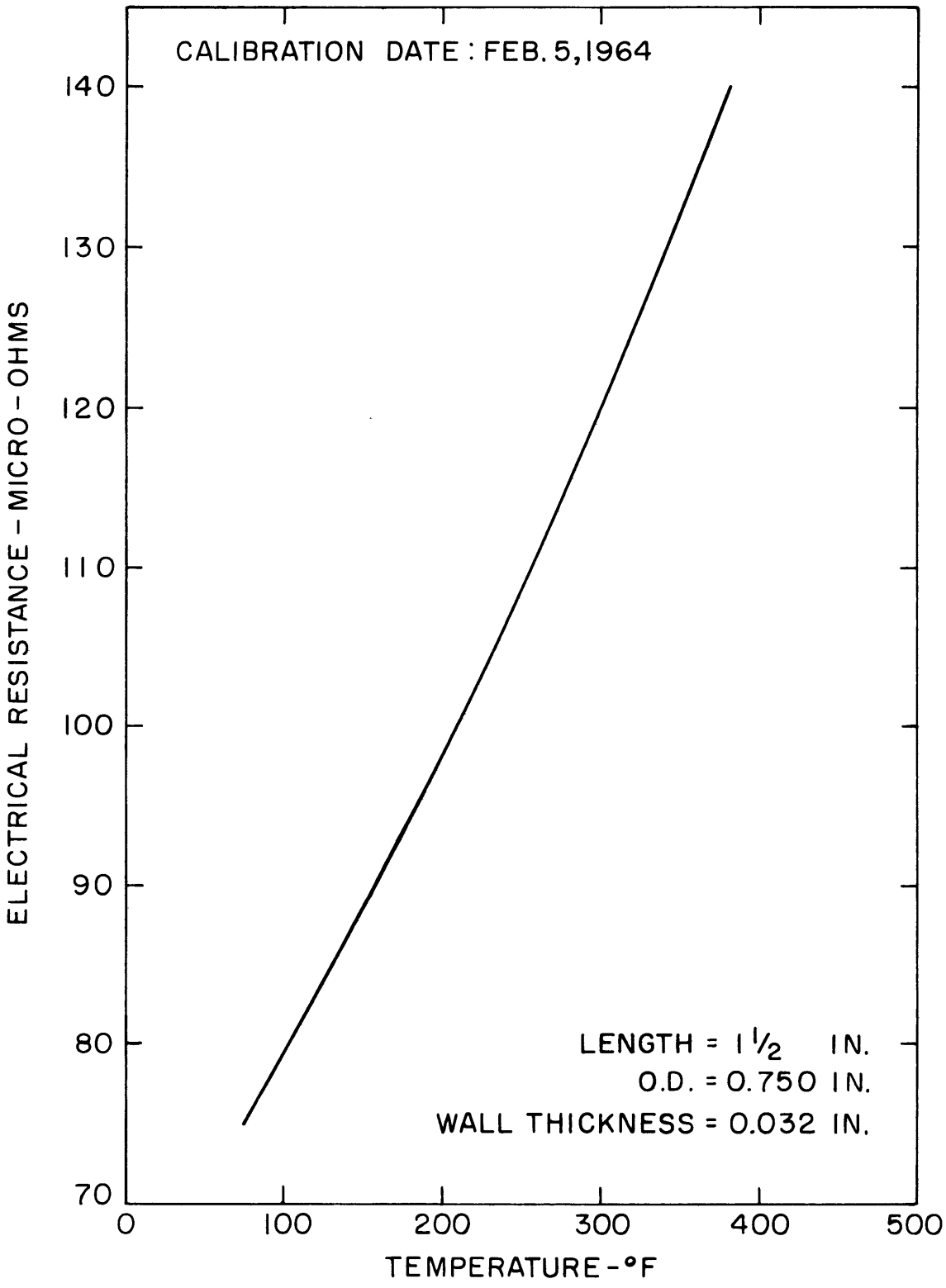

FIG. 11 NICKEL CONDENSER TUBE CALIBRATION

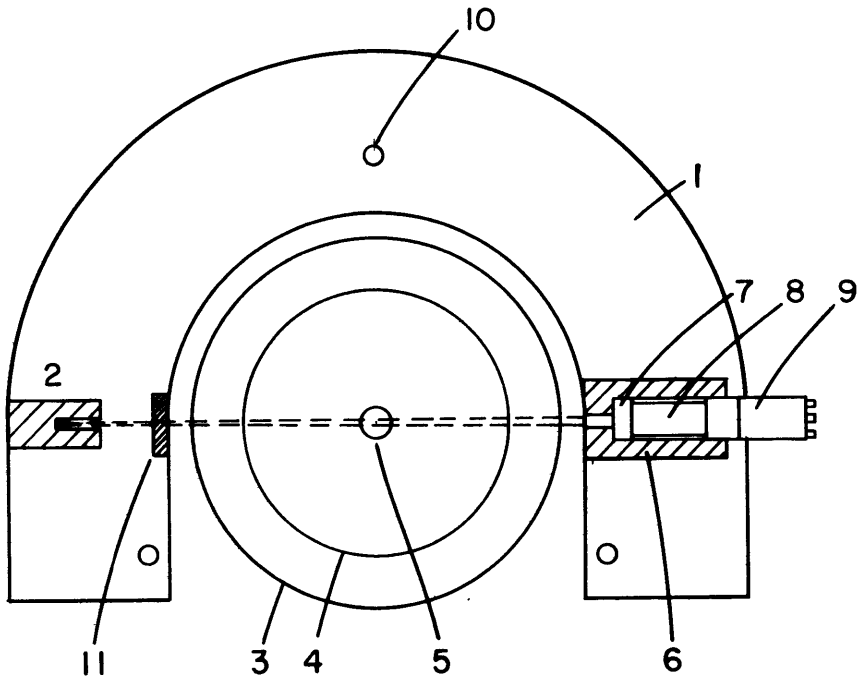

1. ALUMINUM TRAVERSING PLATE
2. CO^{57} SOURCE HOLDER
3. OUTER WALL OF CONDENSING CHAMBER
4. INNER WALL OF CONDENSING CHAMBER
5 NICKEL CONDENSER TUBE
6. LEAD SHIELD ON SCINTILLATION COUNTER
7. SCINTILLATION CRYSTAL
8 PHOTOMULTIPLIER TUBE
9. PRE-AMPLIFIER
10. TAPPED HOLES FOR TRAVERSING MECHANISM
11. POSITION FOR FIXING CALIBRATION DEVICE

FIGURE 12 SOURCE - CRYSTAL ARRANGEMENT

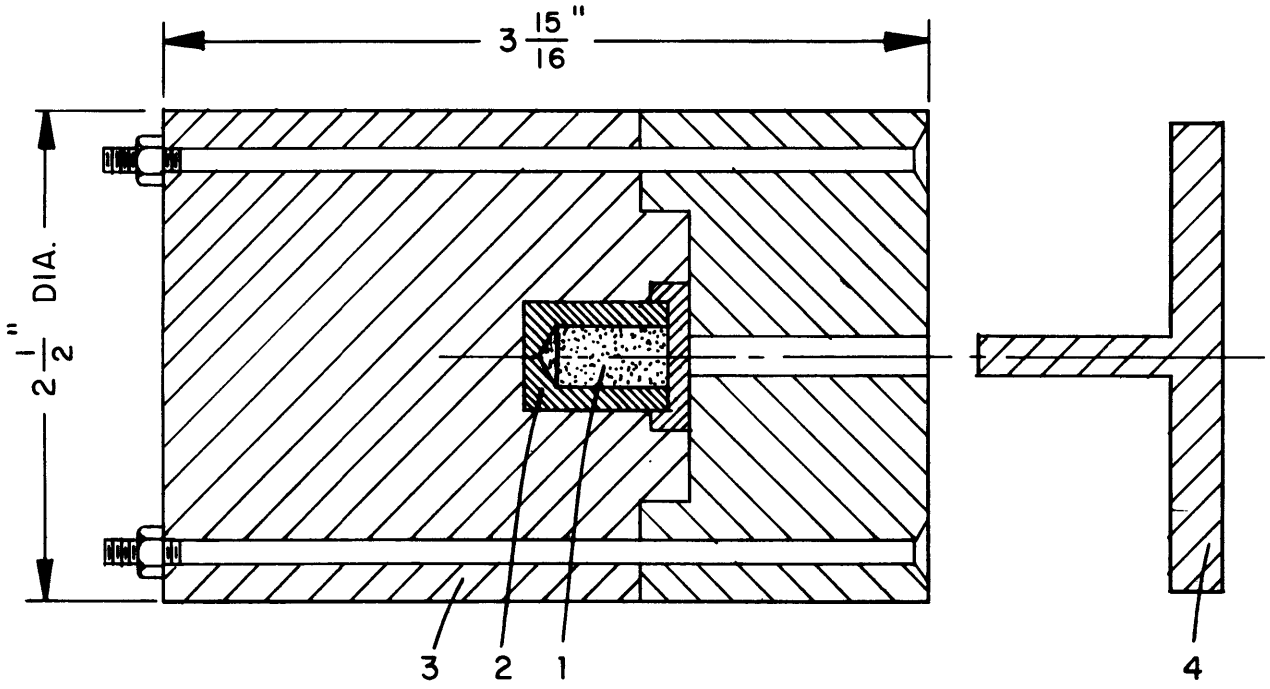

1. CO^{57} SOURCE — 2 mc
2. LUCITE VIAL CONTAINING DRIED SOURCE
3. LEAD CONTAINER
4. LEAD COVER; REMOVED WHILE MAKING MEASUREMENT

FIGURE 13 LEAD HOLDER FOR CO^{57} SOURCE

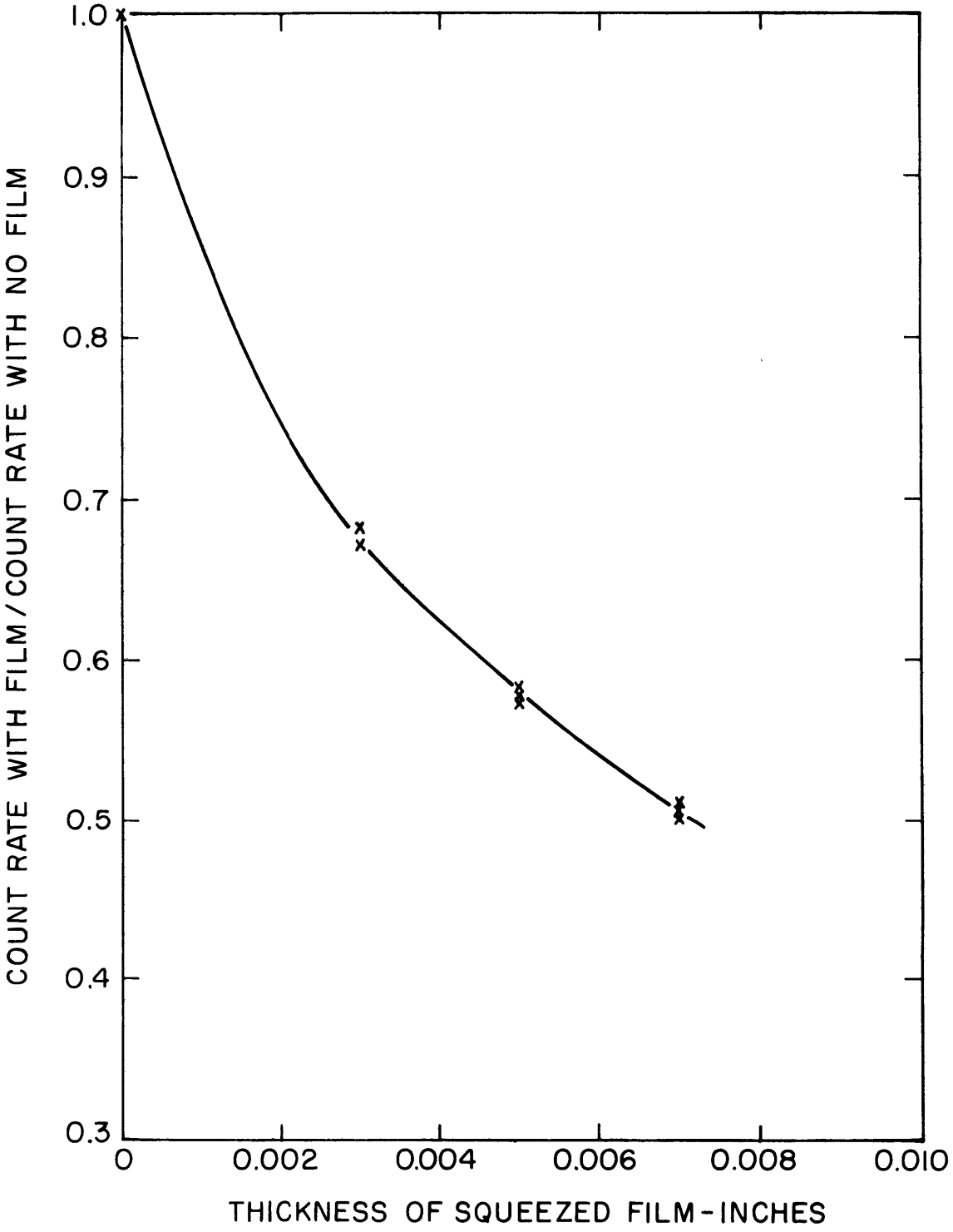

FIG. 14 CALIBRATION PLOT FOR FILM THICKNESS